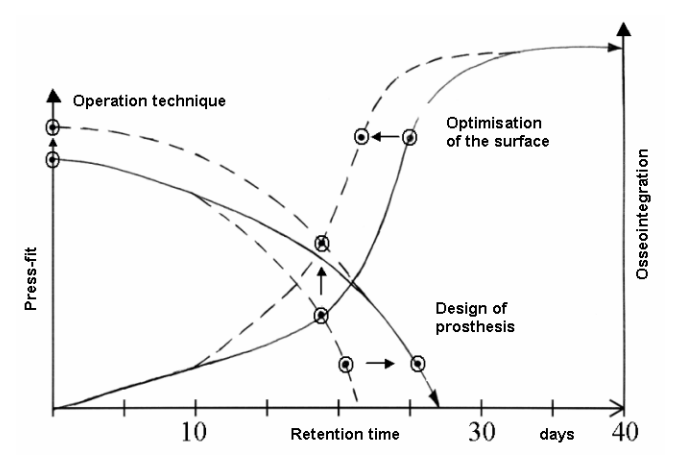
European Cells and Materials Vol. 10. Suppl. 1, 2005 (page 1)

# Plasma spraying for medical application

H. Gruner, Medicoat AG, CH - 5506 Mägenwil

**INTRODUCTION:** For endosseous implant fixation in bone, such as in case of artificial hip and knee joints, two methods are currently applied. The older and more frequent method uses bone cement. Primary fixation of the endoprosthesis is secured by in-situ polymerisation immediately after the implantation.

The second method is the cementless implantation technology. Primary fixation is achieved by mechanical press-fit of the implant into the minimal excavation, well adapted to the geometric configuration of the endoprosthesis.



**Fig. 1.** The change from mechanical (press-fit) to physiological fixation (bony-ingrowth) of a cementless implanted prosthesis as a function of the retention time [1].

The initial degree of press-fit depends on the design of the implant as well as on the performance of the implantation (Fig.1). The long-term stability of the implant is only ensured if the host bone directly interlocks with the surface of the implant. This bonyingrowth must be as fast as possible, because the press-fit-fixation becomes increasingly loose after insertion. Therefore, an optimisation of the implant surface in contact to the host bone is required in order to force the osseointegration.

**SURFACE MORPHOLOGY:** In the past, a variety of surface modifications have been in clinical use. Osseointegration was shown to be fastest and most effective for rough surfaces with open structure that varied between 50 to 400  $\mu$ m [2]. Vacuum Plasma Sprayed (VPS) Titanium coatings are an optimised way to achieve a surface topography and morphology in this preferred 3-dimensional range (Fig. 2). The bone cells anchor directly to Ti due to the presence of a self-protecting  $TiO_2$  passive layer, which is responsible for the biocompatibility of this metal. The individual surface configuration of each type of implant can be engineered within a wide range of roughness to meet the particular requirements for bone bonding at the site of implantation. Responsible

is a careful adaption of the spray powder particle size distribution to the spray parameter. Implants into the less stable spongiosa require a higher roughness compared with the value of a surface in contact to the corticalis.

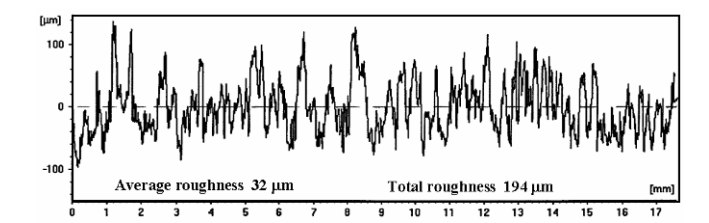


**Fig. 1.** Height profile of a VPS-sprayed titanium coating, recorded with a mechanical stylus profilometer. The thickness of the titanium coating is 350 μm, the surface roughness can be described by the parameters  $R_a$  = 32 μm and  $R_t$  = 194 μm.

**BIOACTIVITY:** Materials that enable an interfacial chemical bond between the implant and the bone tissue due to a specific biological response are called bioactive [3]. Due to its similarity to the mineral phase of natural hard tissue, artificial hydroxyapatite (HA) is considered as a bioactive material.

The idea of using the plasma-sprayed process for the production of HA coatings on endoprosthesis was first described in Japan [4]. In contrast to uncoated metal samples, the implants with HA surface developed in a short time a strong connection between implant and bone tissue. In 1985 the first experience of producing HA coating by the VPS technology was gained [5]. High crystallinity and phase-purity was achieved thanks to a subtile balance between the HA-spray powder and the VPS parameters. The coatings are characterised by a dense and crack-free structure and therefore less prone to penetration of and chemical attack by human liquids.

**CONCLUSION:** The combination of Ti with HA offers an interesting option for a rough surface with osseoconductive approach. The adhesive strength of the ceramic and therefore brittle HA is improved by the ductile Ti undercoat and partially overcomes the discontinuity in mechanical properties at the bone / implant interface. This combination also distributes the mechanical forces across an extended interface belong the rough and significant ductile VPS-sprayed Ti structure down to the stiff metal implant.

### **REFERENCES:**

- [1] Osborn J.S. (1989), Bioceramics EuroAmerica Inc, 388-400.
- [2] Ungethüm M. et al., DVM Proc. 8, 5-15
- [3] Hench L.L. (1971), J. Biomed. Mat. Res. Symp. 2,
- [4] Sumitomo Chemical Co. (1975), Jap. patent application 158745
- [5] Gruner H. (1990), Proc. North Sea Conf. Biomedical Engineering 17-20.
- [6] Ha S.W. (1997), Ph.D. 12198, ETH Zürich.

### Surface modification of biomaterials from an academic research perspective

J. Gold

Department of Applied Physics, Chalmers University of Technology, Göteborg, Sweden

INTRODUCTION: The surface properties of materials in contact with biological systems play a key role in determining the outcome of biological-Properties of particular material interactions. relevance include physico-chemical, topographical, mechanical and bio-functionality. These properties should be considered on the same length scales as the biological entities that are interacting with the material, such as water, biomolecules, cells and organized tissue structures. There are a multitude of surface modification methods available to engineer custom designed interfaces. Many of these methods are not suitable for commercial applications, but can be useful in model studies to investigate the significance of specific aspects of a surface. The optimal surface will vary depending on the particular application, such as location of use for medical implants. More significantly, the optimal surface will vary with time, raising an interest in dynamic surfaces, as well as smart surfaces which react to a changing local biological environment.

**METHODS:** There are many techniques available to modify surfaces. Examples of methods include micro – and nanostructuring of surfaces via various lithographic techniques, imprinting and laser micromaching; shot peening, laser ablation, plasma spraying, gas plasma treatments, ion bombardment, chemical etching, chemical and physical vapor deposition, as well as coatings of polymers, ceramics, metals, molecular self-assembled coatings, as well as biopolymeric coatings of proteins, sugars, lipids, polyelectrolyte coatings and more. Several surface modification methods allowing the production of model test surfaces will be presented, and examples of biological interactions with surfaces made by these methods will also be shown.

RESULTS: Material surface characteristics on µm and nm length scales effect the structure and function of cells and proteins at biointerfaces in vitro. In addition, there are potential synergistic effects of chemical and structural properties on protein and cell behavior. The viscoelastic properties of biomaterial surfaces are being shown to influence cell behavior in vitro and tissue response in vivo. At times in vitro performance of

surface modifications predict an effect in vivo, however in other instances no effect of controlled surfaces are observed. Most likely a multitude of surface properties are acting in concert, and in time, as the biological situation at the interface is so dynamic and versatile.

**DISCUSSION & CONCLUSIONS:** During the past 20+ years, the importance of surface chemistry and topography for medical implants has been recognized and studied. As a result, several new techniques to modify surfaces in a controlled way have been developed or borrowed from other industries. Much research has been conducted to observe and subsequently control biological reactions at surfaces in vitro, and with much success. Unfortunately, the body is a complex environment, and many sophisticated surface modifications that are promising in vitro have shown little or no effect in vivo. A greater understanding of biological processes occurring at interfaces, and more complex in vitro models are required for significant advances in this area.

**ACKNOWLEDGEMENTS:** The Chemical Physics group at Chalmers, The Swedish, Biomaterials Consortium, the SSF Biocompatible Materials Program, the Swedish Research Council, and the Chalmers Bioscience Program.

### "In vitro" evaluation of the composite adhesion to dentine

O. Fodor<sup>1</sup>, I. Tig<sup>1</sup>, M. Moldovan<sup>3</sup>

<sup>1</sup>University of Oradea, Faculty of Medicine and Pharmacy,; <sup>2</sup>Dep. of Dental Materials, "Raluca Ripan" Chemistry Research Institute, 30 Fantanele Street, Cluj-Napoca, Romania

**INTRODUCTION:** The structural complexities of the hard dental tissues, as well as the physical and chemical characteristics of the oral environment are not helping the obtaining of a resistant and long lasting bond. In the adhesive techniques used in dentistry, the most important step is thought to be the adhesion of composites to both enamel and dentin (1,2). The purpose of this study is to evaluate the role and the influence of some dimetacrylic primers upon the adhesion between enamel, dentine and a series of commercial restuarative composite resins.

METHODS Twelve primary caries-free central incisors and premolars were used in the study. All teeth were thoroughly cleaned immediately after extraction and stored in an aqueous solution of 9 % NaCl for up to four months..Standard cavities were prepared as following: on the premolars, standard MOD cavities, being 2mm deep and 4mm wide, and on the central incisors, mesio-vestibulo-distal cavities, being 2mm deep and 4mm wide. Each cavity was performed using a water-sprayed, highspeed handpiece with new diamond-coated burs Each cavity was cleaned and dried. The cavities were then filled with a composite resin and his adhesiv system, according to the manufacturer's instructions: Point 4+Optibond SoloPlus ( Kerr ), Synergy+One Coat SE Bond (Coltene), Admira +Admira Bond (Voco) and CF1 + C-Bond (Willmann&Pein). The composite autochthon CF1 were, by weight, 80% filler's and 22% resin composed of 65% Bis-GMA and 35% TEG-DMA 0.5% CQ, 1% DMAEM and the polymerization inhibitor BHT. The filler was both 80 % strontium glass and 20% colloidal silica. All teeth were then vertically sectioned into 3 mm thick halves with water-cooling, using a precision cutting instrument with a diamond disc. After cleaning, the samples were stored in distilled water and examined in various magnifications with a Philips L 20 scanning electron microscope.

RESULTS The quality of the restorations was evaluated by both direct and indirect methods. The SEM studies partially confirmed the clinical observations. In fig.2 the bond between the composite resin, enamel and dentine can be seen. The SEM analysis provides useful information about many areas of the adhesive-dentin interface. At the enamel-composite resin interface a very good bond can be observed. When using the self-etch primer adhesive, the formation of the hybrid layer on the top of the dentine substrate can not be observed, but we can see the infiltration of the smear layer. In contrast, when using a separate etching adhesive system we can observe the

formation of a hybrid layer and a better sealing of the dentine/composite resin gaps.

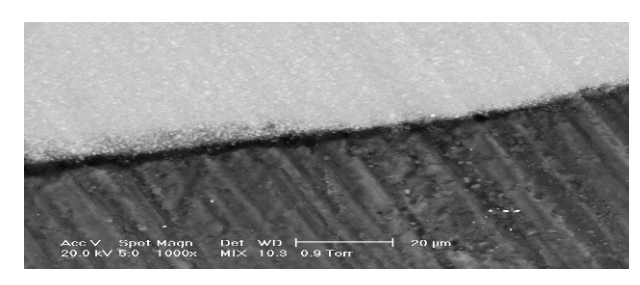


Fig. 1 Restoration with Admira and Admira Bond (Voco. Section visualised using the SEM



Fig.2. Restoration with Synergy and One Coat SE Bond . Section visualised using the SEM

### **DISCUSSION & CONCLUSIONS:**

Composite materials are a viable solution for direct restoration of the anterior and posterior teeth, with positive results on medium and long term, if manufacturer's instructions and the clinical indications are respected. The system that we have tested 'in vitro', offers o good adhesive bonding between the composite resin, enamel and dentin. To sum up, we can say that for the self-etching

primer adhesive system, the strength of the adhesive bond is given by the the adhesion of the smear layer to the dentine, while the adhesive system that are using separate etching, form a hybrid layer on the top of the dentine substrate, which leads to a superior strength of the adhesive bond.

**REFERENCES:** D.H. Pashley, R.M. Carvalho (1997), *Dentine Permeability and dentine adhesion*, Journal of Dentistry, Vol.25, Nr.5, pp. 355-372; J.D. Eick, A.J.Gwinnett, D.H.Pashley, S.J.Robinson (1997), *Current concepts on adhesion to dentin*, Crit Rev Oral Biol Med, Vol.8, nr.3, pp. 306-335

**ACKNOWLEDGEMENTS**: D-na M. Moldovan, Dep. of Dental Materials, "Raluca Ripan" Chemistry Research Institute, 30 Fantanele Street, Cluj-Napoca, Romania

# POLY (PROPYLENE SULFIDE)-BL-POLY (ETHYLENE GLYCOL), (PPS-PEG), ON GOLD: A STEP TOWARDS SURFACE MODIFICATION IN BIOSENSOR RESEARCH

L. Feller<sup>1, 2</sup>, S. Cerritelli<sup>2</sup>, M. Textor<sup>1</sup>, J. Hubbell<sup>2</sup>, S. Tosatti<sup>1</sup>

ETH Zürich, Zürich, Switzerland. <sup>2</sup> EPF Lausanne, Lausanne, Switzerland.

**INTRODUCTION:** The use of *in situ* biosensors in different bio-related fields have gained importance in the past years, because of the need of being able to monitor processes occurring among different biological based species or analyzing composition of a given compound. In order to improve the sensitivity of such biosensors, their surface has to be designed and engineered in a manner that the amount of non-specific event is minimized. The use of PEGylated surfaces has been often considered in this respect. Thereafter, the present study is aspired to improve the control of non-specific interactions between the biosensor surface and the analyte by use of PEG based monomolecular coatings. In our approach, a block copolymer containing one (di- block) or two (triblock) PEG chains separated by a poly (propylene sulfide) (PPS) part is used. Once PPS-PEG is adsorbed onto gold surfaces, a stable linkage between the sulfur atoms of the PPS thioether and the metal surface is observed. The hydrophilic PEG part forms a dense PEG brush, exposed to the aqueous environment and passivates the surface against protein adsorption. It has been shown that PPS-PEG is more stable to oxidation than singlesite attached alkanethiolates [1].

METHODS: In this study, different architectures of di- and tri-block PPS-PEG copolymers were synthesized [2], characterized, and deposited on gold substrates. While the PPS part was kept constant (about MW 4000), the PEG part was varied between 1100 and 5000 Da molecular weight in order to obtain different ethylene glycol (EG) surface densities and so tailor the degree of protein surface interactions. The formation of a chemisorbed adlayer was monitored by Surface Plasmon Resonance (SPR), *ex situ* ellipsometry and X-ray Photoelectron Spectroscopy (XPS). Resistance of the surfaces towards protein adsorption was evaluated *in situ* by SPR.

**RESULTS:** SPR measurements provide good evidence that the mass of proteins adsorbed from serum solution depends on the architecture of the adsorbed polymer as shown when plotting the adsorbed mass of proteins as a function of the density of ethylene glycol monomeric units (EG) (Figure 1). In general, less adsorption of serum is observed in presence of a PPS-PEG adlayer. Triblocks are more effective than di-blocks in

rendering a surface protein resistant. The lowest adsorption was observed for 2k/4k/2k. In comparison to a bare cleaned gold substrate the serum adsorption is lessened to 96.7% [3].

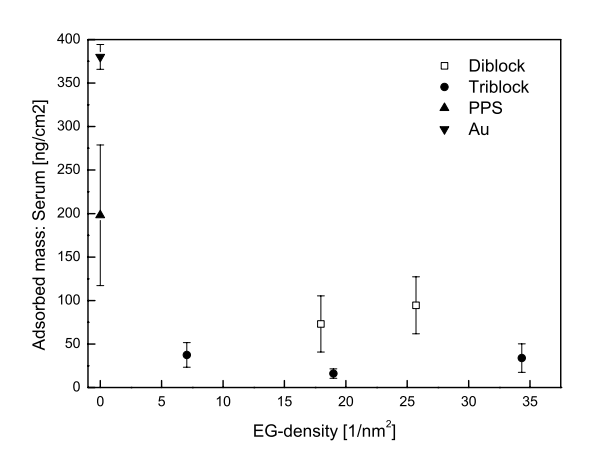


Fig. 1: Mass of serum [ng/cm²]that adsorbs onto PPS-PEG-coated gold surfaces upon exposure to human serum for 30 min and subsequent rinsing in 10 mM HEPES buffer (pH 7.4) as a function of the EG monomer surface density. The adsorbed protein mass was determined by SPR; the EG monomer surface density was determined from the adsorbed polymer mass (SPR) and the NMR-determined polymer architecture of the bulk polymer.

DISCUSSION & CONCLUSIONS: The data indicated a close relationship between protein adsorption resistance and polymer architecture, resulting in adlayers with different ethylene glycol surface densities. This last parameter seems to be the key factor in respect of protein resistance. This hypothesis is sustained from the results obtained by comparing our experimental protein adsorption data with values reported in the literature and confirms the tendency of a platform-independent response of PEGylated surfaces. Among the different possibilities to passivate gold surfaces, PPS-PEG based adlayers have then shown to be a highly interesting technique considering their high stability and their protein resistance.

**REFERENCES:** <sup>1</sup>J. P. Bearinger et al. (2003) Nature Materials, **2**:259-264. <sup>2</sup> A. Napoli et al (2001) Macromolecules **34**: 8913-8917. <sup>3</sup> L. Feller et al (2005) in preparation.

**ACKNOWLEDGEMENTS:** We thank Samuel Terrettaz at EPF Lausanne, Janos Vörös and Laurent Feuz, ETH Zürich.

### Disinfection of Silicone Surfaces using Photo-Activated Disinfection

T.B. Gallagher<sup>1</sup>, G.W. Hanlon<sup>1</sup>, A.W. Lloyd<sup>1</sup>, J-Y. Maillard<sup>2</sup>

1. School of Pharmacy and Biomolecular Sciences, University of Brighton, Brighton, England 2. Welsh School of Pharmacy, Cardiff University, Cardiff, Wales

### **INTRODUCTION:**

As current antimicrobial agents are gradually being rendered ineffective by resistance developing in target organisms there is an urgent need for alternative antimicrobial approaches. Toluidine Blue O (TBO) is a light-activated antimicrobial agent which has been shown to be effective against a wide range of bacteria. The aim of this investigation was to determine the efficacy of TBO against biofilms grown on silicone surfaces when impregnated into the substrate and when applied externally.

### **METHODS:**

Silicone discs were impregnated with 1mg/ml TBO by swelling the discs with chloroform for two hours and then applying the TBO solution (or water for controls) for 16 hours. The discs were then rinsed of excess TBO and dried. Biofilms of *Proteus mirabilis* and *Staphylococcus epidermidis*-were grown by seeding the silicone discs for four hours with the appropriate culture in TSA at 37°C (1x10<sup>5</sup> CFU/ml). The culture was then removed from each disc and replaced with fresh medium. The discs were then incubated for a further 44 hours.

PAD was initiated by activating the biofilms for 15 minutes with red light from a diode laser (wavelength:  $633 \pm 2$ nm) to apply a total energy does of 59 Joules. In an alternative treatment protocol discs were washed with a TBO solution (25µg/ml) followed by light activation as before.

Following treatment biofilm viability was assessed by removal of adherent bacteria and enumeration by viable counts.

### **RESULTS:**

For *S. epidermidis* biofilms washing with TBO led to a 3.2 log reduction in cell numbers. Impregnated discs when not exposed to red light resulted in a 1.1 log reduction and when exposed to red light a 1.2 log reduction was observed. Washing of biofilms grown on impregnated discs gave a 1 log reduction in the non-light-activated control and a 2.4 log reduction when exposed to red light (wavelength:  $633 \text{nm} \pm 2$ ).

For *P.mirabilis* biofilms washing alone led to a 1.1 log reduction in cell numbers when compared to the controls. Impregnated discs when not exposed to red light gave a 0.4 log reduction and when exposed to red light no further reduction was observed. Washing *P.mirabilis* biofilms on

impregnated discs gave no significant reduction in the control (0.1 log) and a 1 log reduction when exposed to red light.

### **DISCUSSION & CONCLUSIONS:**

Successful disinfection according to the British Standard (BS EN 1276)<sup>1</sup> occurs when there is a five log reduction in cell number within 5 minutes. This did not occur with any of the treatment protocols described here.

When the two organisms are compared, it can be clearly demonstrated that *S. epidermidis* is more susceptible to disinfection using PAD than *P. mirabilis*. However, this was to be anticipated as most research suggests that Gram negative bacteria are more resistant to this mode of killing than Gram positive bacteria<sup>2</sup>.

However, it was unexpected that the discs which had been impregnated with TBO showed a reduced kill level when compared to biofilms which had only been washed with TBO.

Two main conclusions can be drawn from this investigation:

- Gram positive organisms are more susceptible to killing using singlet oxygen than Gram negative organisms.
- Treating biofilms with an externally applied solution of TBO is a more successful method of applying PAD technology than release of impregnated TBO.

### **REFERENCES:**

<sup>1</sup> British Standard. Chemical disinfectants and antiseptics - quantitative suspension test for the evaluation of bactericidal activity of chemical disinfectants and antiseptics used in food, industrial, domestic and institutional areas - Test method and requirements (phase 2/step 1). BS EN 1276: 1997.

<sup>2</sup> Bonnett, R., Evans, R., & Galia, A. 1997, "Immobilised Photosensitisers: Photosensitiser films with microbicidal effects", *Proc.Soc.Photoopt Instrum Eng.*, **3191:** pp. 79-88.

### **ACKNOWLEDGEMENTS:**

TG was financially supported through an EPSRC CASE studentship with Denfotex Ltd. The project team are also grateful for the academic and technical support provided by the company.

### EFFECTS OF TIMAX™ ON GROWTH AND DIFFERENTIATION OF HUMAN OSTEOBLAST-LIKE CELLS UNDER SERUM-FREE CULTURE CONDITIONS

I. Gerber<sup>1</sup>, S. Koch<sup>2</sup>, T. Zehnder<sup>3</sup>, J. Mayer<sup>4</sup>, T. Wallimann<sup>1</sup>, M. Textor<sup>5</sup>, L. Faber<sup>6</sup>, S. Mikailov<sup>3</sup>

<sup>1</sup> Institute of Cell Biology, ETH Hoenggerberg, 8093 Zurich; <sup>2</sup> MSRU, Animal Hospital, 8057 Zurich; <sup>3</sup> CAFI, 2400 Le Locle; <sup>4</sup> TECIM, 5702 Niederlenz; <sup>5</sup> LSST, ETH Hoenggerberg, 8093 Zurich; <sup>6</sup> DePuy ACE, 2400 Le Locle

### INTRODUCTION:

Primary human osteoblast-like cells (HOB) are used because the differentiation pattern is not identical to the one observed in the rat system or in cell lines.

### **METHODS:**

HOB were isolated from randomly collected bone chips of patients under going total hip replacement surgery. Identical cell numbers per dish (1.25x10<sup>4</sup> cells/cm<sup>2</sup>) were used for culturing these cells in monolayer and as micromass cultures. Bone chips and isolated cells, were kept under serum-free conditions during the entire culture time. The growth medium was supplemented with ascorbate and 1,25dihydroxyvitamin D<sub>3</sub>. TiMAX™ and 4 modified surfaces of TiMAX™ (S1, S2, S4 S5) were compared as cell substrates to reference material such as stainless steel (316L), Ti-6Al-4V (TAV), commercially pure titanium with surfaces as received, as well as roughened and polished (cpTi, cpTir, cpTip respectively). TiMax is Ti6Al4V that has been anodized with a proprietary process. The standard culture dish surface was used as control. The materials were provided by DePuy ACE. At various time points, cel1 adhesion (immunolfluorescence localization of vinculin), morphology (SEM), viability (neutral red uptake), metabolic activity (MTT assay), and cell number (DNA) were analyzed. Differentiation was assessed by alkaline phosphatase activity (ALP), collagen content, secretion of C-terminal propeptide of type I collagen (CICP), and osteocalcin (OC) secretion.

### **RESULTS:**

After 3 days in culture, the cells in the central area of a micromass formed a dense, multilayered tissuelike structure, whereas the cells in monolayer were clustered or 'island-like' distributed. The cells established many cell-cell contacts over long and short distances. At 2 weeks, HOB were forming multilayers with a dense network of abundant cell processes and filopodia. The cells were separated by collagen fibrils in the extracellular matrix, which consisted mainly of type I collagen, some collagen type III, and little type V. In addition, the staining of all cells and dead cells as well as the immunofluorescent localization of focal adhesion sites were all similar in the cells grown on the various metals, although no quantitative analysis was done.

Monolayers were significantly lower than micromasses in total NR uptake, metabolic activity, cell number as well as all differentiation parameters at a cellular level, but metabolic activity and protein content per cell were not affected.

TiMAX and S1 clearly promoted cell growth over 316L followed by TAV and the cpTi groups. There were no significant differences found between TiMAX and the new modified surfaces. Concerning the differentiation parameters, such as ALP, CICP, collagen and OC, which were expressed per cell or cellular activity, S1 and TiMAX are also clearly stimulating differentiation over 316L, TAV and all cpTi groups. The effects of S5 and S2 are less pronounced than those of TiAMX and S1, but higher than S4. The multiplication of the values per dish for viability, metabolic activity, collagen and osteocalcin is a valuable parameter to get concomitant information for proliferation and differentiation. Overall TiMAX and S1 behave significantly better than 316L, cpTi and TAV. S2 and S4 score significantly higher than 316L. In addition, S2 is better than TAV. S4 is significantly lower than S1.

### **DISCUSSION & CONCLUSIONS:**

The effects of the metals were independent of the culture system used, which means that cell-cell contacts did not influence the reactions of HOB to the metal substrates. The micromass culture system, which represents an organoid system, did not show the same beneficial effects on differentiation as was seen with juvenile rat calvarial osteoblasts <sup>1,2</sup>.

As a general conclusion from investigating all individual parameters, mainly TiMAX and S1, and to a lesser extent S5, S2 and S4, are promoting not only HOB growth but also their differentiation over 316L followed by TAV and the cpTi group. The roughness of cpTi had only minor effects on these parameters.

### **REFERENCES:**

- 1. Gerber, I. & ap Gwynn, I. Eur Cell Mater **2**, 10-20. (2001).
- 2. Gerber, I. & ap Gwynn, I.. Eur Cell Mater 3, 19-30 (2002).

**ACKNOWLEDGEMENTS:** This project was supported by a CTI grant and DePuy ACE, Le Locle. d by a CTI grant and DePuy ACE, Le Locle.

# Surface modification of titanium based alloys with bioactive molecules utilizing electrochemically fixed oligonucleotides

D. Scharnweber<sup>1)</sup>, J. Michael<sup>2)</sup>, R. Beutner<sup>1)</sup>, I. Israel<sup>2)</sup>, U. Hempel<sup>3)</sup>, B. Schwenzer<sup>2)</sup>, H. Worch<sup>1)</sup>

1) Max-Bergmann-Zentrum für Biomaterialien, 2)Institut für Biochemie, 3)Institut für Physiologische Chemie; all Technische Universität Dresden, Dresden, Germany

**INTRODUCTION:** Though titanium based alloys are used in routine surgery, problems arise from special medical indications, for example bad local bone quality or systemic diseases. Here, a method for bio-surface engineering of implants in a modular way is presented, offering the possibility to adapt biochemical surface properties specifically prior to implantation.

In a first step an oligonucleotide that acts as anchor group (AON) is fixed via one terminus (regiospecifically) by partial electrochemical entrapment into anodic oxide layers. This AON is subsequently hybridized with a complementary oligonucleotide (CON) conjugated to bioactive molecules. This staged process enables flexibility and modularity of the system based on the hybridization ability of nucleic acids.

**METHODS:** Samples of Ti6Al7Nb (Synthes Inc.) were grinded and etched (HF/HNO<sub>3</sub>). Oligonucleotides (Thermo Electron Corp.) were partially <sup>32</sup>P-labelled by Hartmann Analytic GmbH. Amounts of ON on the surface were determined using a PIPS spectrometer system (Canberra / Ortec).

Immobilization of a 60mer, 5'-phosphorylated anchor strand (AS) was performed in acetate buffer (pH = 4.0) up to potentials of 15  $V_{SCE}$ . Stability of fixation was tested by immersion in 50 mM TRIS-HCl (pH = 7.5) for up to 24 h. Hybridization experiments with 31mer complementary (CS) and non-complementary (NS) strands to AS, respectively, were carried out in the same electrolyte. Hybridization was performed in two steps of 30 min each (without/with 10 mM MgCl<sub>2</sub>).

Conjugates were synthesized from a cell adhesion peptide (GRGDSP, Bachem) and CS according to Ruth [1]. Bioactivity of the conjugates was tested by blocking the integrine receptors of rat-calvaria osteoblasts (<sup>3</sup>H-labelled) with GRGDSP alone and with its conjugate, respectively, before seeding on polystyrene cell-culture plates.

**RESULTS:** During immersion of AS coated samples for up to 24 h merely adsorbed ON desorb to a large extent (fig. 1). Anodic oxidation with potentials of at least 4  $V_{SCE}$  leads to stable fixation. After desorption up to 43 % (14.5  $V_{SCE}$ ) of the amount of ON detected after immobilization was present at the surface, hence fixed. A maximum surface density of 4 pmol/cm<sup>2</sup> after desorption

could be achieved by immobilization from 400 nM AS solution at a potential of 8  $V_{\text{SCE}}$ .

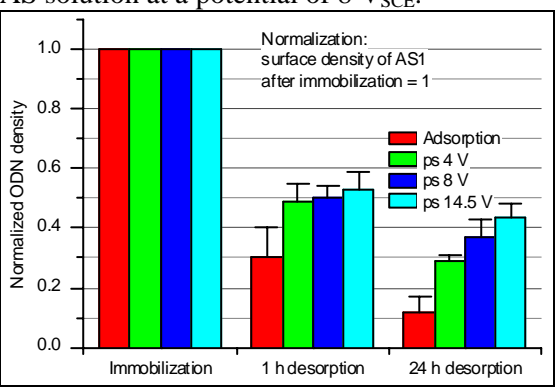


Figure 1: Normalized AS density on the surface after immersion in 50 mM TRIS-HCl (pH = 7.5)

Hybridization efficiency depends on the surface density of immobilized anchor strand and reaches values of up to 1.0. Addition of MgCl<sub>2</sub> increased hybridization rates.

Similar hybridization behaviour was exhibited by the conjugates. The successful binding of the conjugates to integrins of osteoblasts could be demonstrated.

DISCUSSION & CONCLUSIONS: Oligonucleotides can be fixed stably in anodic oxide layers on titanium based alloys and remain accessible for hybridization with complementary strands. Hybridization of a conjugate of complementary strand and RGD peptide with the fixed anchor strands is possible to the same extent as for the non-conjugated strand. Furthermore, the cell adhesion peptide preserves its binding capabilities to integrine receptors of osteoblasts if conjugated to ON. All results clearly indicate that modular implant adaptation as introduced above is possible.

**REFERENCES:** [1] Ruth JL. Conjugation of enzymes to linker arm oligodeoxynucleotides. In: Eckstein F, editor. Oligonucleotides and Analogues. IRL Press, 1991. p. 270 et sqq.

**ACKNOWLEDGEMENTS:** Financial support of the DFG (WO494/14 and SCHW638/3-1) is greatly acknowledged. The authors thank Synthes, Inc. for providing the Ti6Al7Nb alloy.

# Rheological Behaviour of some Cross-linked Collagen Hydrogels for Drug Delivery Use

M G Albu<sup>1</sup> & M Leca<sup>2</sup>

Leather and Footwear Research Institute, 93 Ion Minulescu Str., Bucharest

**INTRODUCTION:** Due to the binding capacity, type I fibrillar collagen is extensively used as delivery systems for drugs [1, 2]. To increase hydrogel viscosity, increase the mechanical strength of the corresponding membranes or porous matrices and control biodegradability, hydrogels are crosslinked with different agents, usually formic or glutaric aldehydes<sup>1</sup>. The object of this paper is the crosslinking of type I fibrillar collagen hydrogel with different amounts of formic or glutaric aldehyde and rheological characterization of the resulted hydrogels, high consistency of hydrogels being important when matrices are obtained.

**METHODS:** Type I fibrillar collagen hydrogel 0.6% w/w, extracted from calf hide by basic and acid treatments at  $22^{\circ}$ C using hydrochloric acid, was crosslinked with 0.005-0.015% (reported to the amount of collagen) formic or glutaric aldehyde in the following conditions: pH = 8.2,  $4^{\circ}$ C, 24 h.

Rheological measurements were made at  $25\pm0.1^{\circ}\text{C}$  using a Haake RT 550 Viscotester developing shearing rates ranging between 3 and  $1312~\text{s}^{-1}$  and measuring apparent viscosities between 0.15 and 1000 Pa.s.

**RESULTS:** The rheograms of the initial and crosslinked hydrogels are shown in Figure 1a, b.

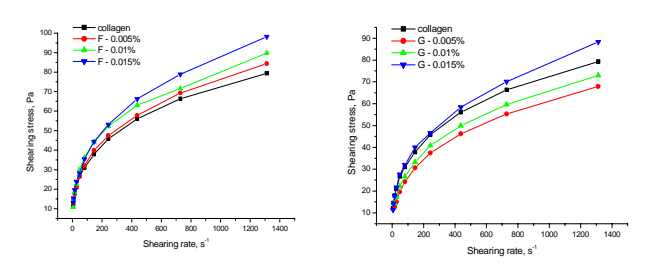


Fig.1: Rheograms of 0.6% type I fibrillar collagen hydrogel containing the specified amounts of: a) formaldehyde; b) glutaraldehyde

The dependence of viscosities at zero shearing rate on the concentration of the two aldehydes is shown in Figure 2a, b.

**DISCUSSION & CONCLUSIONS:** Both the rheograms obtained for the initial hydrogel and for

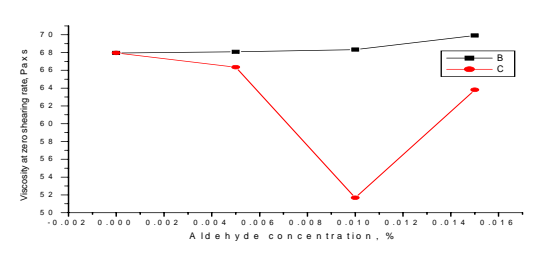


Fig.2: Dependence of viscosities at zero shearing rate on aldehyde concentration: B – formaldehyde; C – glutaraldehyde

those containing the two crosslinking agents (Fig. 1a, b) show a pseudoplastic behaviour.

When formaldehyde was used as a crosslinking agent the hydrogels have a homogenous appearance for all the studied collagen/aldehyde ratios and the shearing stresses increase with crosslinking agent concentration at all the shearing stress. This demonstrates the increasing of hydrogel consistency as a result of crosslinking. But the viscosities at zero shearing rate,  $\eta_{\rm o}$ , increase only slightly with formaldehyde concentration (Fig. 2B) due to the hydrogel destruction at higher aldehyde content.

Using glutaraldehyde the hydrogels are more viscous, especially for the last two concentrations. It is homogenous for 0.005% aldehyde and look pretty discontinuous for the other concentrations. In addition, the rheograms are placed under the collagen one for 0.005 and 0.010% aldehyde and above it for 0.015%. This difference is reflected in the dependence of  $\eta_{\rm o}$  on aldehyde concentration: it is very close to that of the initial hydrogel for 0.005% aldehyde, decreases drastically for 0.010% due to the destruction of hydrogel structure and increases again for 0.015% due to the high increase of hydrogel consistency.

The differences in viscosity and homogeneity of the hydrogel crosslinked with the two aldehydes can be explained by the complex crosslinking mechanism when glutaraldehyde is used.

**REFERENCES:** <sup>1</sup>W. Fries (1998) *Eur. J. Pharm.* & *Biopharm.* **45**:113-136. <sup>2</sup> C.H. Lee, A. Singla, Y. Lee (2001) Int. *J. Pharm.* **221**:1-22.

<sup>&</sup>lt;sup>2</sup> University of Bucharest, Physical Chemistry Dpt., 4-12 Regina Elisabeta Blvd., Bucharest

### Surface modification to direct biological response to inorganic materials

### Marcus Textor

ETH Zurich, Department of Materials, Laboratory for Surface Science and Technology, BioInterfaceGroup, Wolfgang-Pauli-Strasse 10, CH-8093 Zurich, Switzerland

The spontaneous assembly of multifunctional molecules at surfaces has become a useful technique to design hybrid interfaces for the biosensor field, model surfaces for cell-biological studies and drug carrier surfaces for medical application. While alkanethiol self-assembled monolayers on gold surfaces are routinely used today, there is a need for a wider range of reliable assembly systems that are compatible with oxide-based substrate surfaces. The general objective is to produce interfaces via cost-effective, robust techniques that allow the elimination of non-specific protein adsorption ("non-fouling" surfaces) and the addition of bioligands at controlled surface density and molecular conformation in order to direct the biological response to biomaterials and biosensor chips.

Poly(ethylene glycol)-grafted polyionic copolymers assemble spontaneously from aqueous solutions at charged interfaces resulting in well-defined, immobilized monolayers or multilayers depending on the polymer architecture. The degree of interactiveness can be controlled quantitatively through the design of the polymer architecture. If the polymer is functionalized with bioligands such as peptides (to mimic cell-interactive proteins), biotin (link to (strept)avidin) or NTA-Ni<sup>2+</sup> (link to histidin-tagged biomolecules), biomaterial and biosensor interfaces with quantitative control over ligand density can be efficiently produced.

Chemical patterning of surfaces into (bio)adhesive and non-adhesive areas in the micrometer to nanometer range has become an important tool to organize biological entities such as cells and biomolecules at interfaces in a highly controlled manner. Two novel surface modification techniques are presented that combine conventional microfabrication (top-down) with molecular self-organization (bottom-up approach). Biologically meaningful patterns of protein-adhesive and non-adhesive areas in a size range from micrometers to as small as 50 nm could be produced with consistent quality and on comparatively large areas (e.g., whole 4-inch wafers).

Fluorescence microscopy, XPS, ToF-SIMS, Ellipsometry and AFM were used to control *ex situ* each surface modification step, while the kinetics of the interface reactions including the interaction with biological media were monitored *in situ* with an optical, evanescent field based sensor (OWLS) and the quartz crystal microbalance (QCM-D) technique.

Poly(L-lysine)-graft-poly(ethylene glycol) Assembled Monolayers on Niobium Oxide Surfaces: A Quantitative Study of the Influence of Polymer Interfacial Architecture on Resistance to Protein Adsorption by ToF-SIMS and in situ OWLS. S. Pasche, S.M. De Paul, J. Vörös, N.D. Spencer and M. Textor, Langmuir 19(22): 9216-9225 (2003)

Selective Molecular Assembly Patterning: A New Approach to Micro- and Nanochemical Patterning of Surfaces for Biological Applications. R. Michel, J.W. Lussi, G. Csúcs, I. Reviakine, G. Danuser, B. Ketterer, J.A. Hubbell, M. Textor, N.D. Spencer, Langmuir 18(8): 3281-3287 (2002)

Nanometer-thin, Soft Polymer Cushions: A Novel Coating on Chips for the Analysis of Genes and Proteins. J. Vörös, S.M. De Paul, A. Abel, M. Pawlak, M. Ehrat, M. Textor, Bioworld 2: 16-17 (2003)

Use of Molecular Assembly Techniques For Tailoring the Chemical Properties On Smooth and Rough Titanium Surfaces. M. Textor, S. Tosatti, M. Wieland and D.M. Brunette, «Bio-Implant Interface: Improving Biomaterials and Tissue Reaction», Editors: Ellingsen & Lyngstadaas, CRC Press, 2003.

### The structure, composition and visual opacity of some dental composite resins C. Alb<sup>1</sup>, M.Manole<sup>1</sup>, S. Alb<sup>2</sup>, M. Moldovan<sup>3</sup>, D. Dudea<sup>1</sup>

Dept. of Dental Materials and Prosthodontics, University of Medicine and Pharmacy "Iuliu Hatieganu",

**INTRODUCTION:** The continuous effort of both researchers and producers in the field of dental restorative materials to improve their properties as well as their clinical success rate is revealed by the constant changes of the filler in the composite resin. The modern fillers included in the latest materials are based on radioopaque elements which allow the dentist to detect secondary caries, but also influence the optic properties, thus the esthetic result of these restorative materials. [1-2] The purpose of this study was to evaluate and compare the structure, composition and visual opacity (translucence) for commercial dental materials.

**MATERIALS & METHODS:** We have studied six commercial composite resins containing irregular-shaped fillers as experimental materials. Table 1. Composite resins examined in this study

Materials	Manufacturer		
Tetric Ceram(C1)	Vivadent Schaan, Liechtenstein		
Composite autohton (C2)	Remed Prodimpex, Cluj-Napoca Romania		
Spectrum (C3)	Dentsply De Trey, Konstanz, Germany		
Charisma (C4)	Kulzer, Friedrichsdorf, Germany		
Solitaire 2 (C5)	Heraeus Kulzer, Wehrheim, Germany		
Compoglass (C6)	Vivadent Schaan, Liechtenstein		

Characterization of the composite resins The composition and structure of the six materials were examined using a Philips L 20 scanning electron microscope. Specimens for scanning electron microscope (SEM) observation of the ground surface texture were prepared by filling composite resins into a Teflon mould (6 mm width, 3 mm thickness) and were kept in distilled water at 37°C for 24 hours. Other specimens were prepared in disc-shaped Teflon moulds (2 mm thickness) for measuring the translucency of the composite resins by spectral investigations UV-VIS using a spectrophotometer type UNICAM 4 UV-VIS (574 nm and 800 nm).

**RESULTS & DISCUSSION:** The photographs taken under the microscope showed that the studied composite resins have a similar microstructure, the variations between the six investigated commercial composites are not significant. We have observed a very homogeneous structure at the C4 composite resin, filled with Ba-Al-Si glass, with some bigger size particles with sharp edges. The presence of  $SiO_2$  in the C4 showed us the filler size varies between  $0.01\text{-}0.07~\mu m$  and  $0.04~\mu m$ . The qualitative analysis

of the studied materials has revealed the presence of the ions Ba, Ca, Al, Si, Zn thus proving the composition that was considered when they were produced. From the SEM observations we have concluded that all six materials have the filler particles dispersed. These materials have a constant distribution of the particles, while other composite resins have a filler distribution in a wider specter, which leads to improves characteristics regarding consistence and plasticity. The translucence may vary upon the specific applications of the dental restorative materials. Our study has evaluated the translucency of all the six composite resins in order to determine the effect of the chemical composition of the resins upon their translucence. The results showed the changes in the transmittance along with the increase of the wave length. The values of the transmittance for the tested materials under 2 wave lengths on white and black background are resumed in Figure 1.

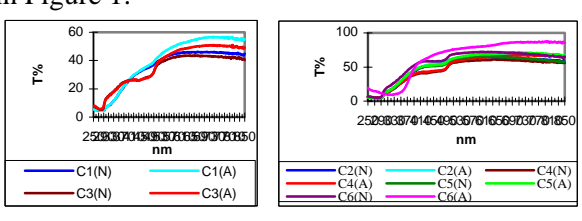


Figure 1. Spectra UV-VIS for dental composites

The resins containing Ba glass particles or a mixture of Ba and Ytterbium glass have lower values of the transmittance as compared to those with Zn glass filler.

CONCLUSIONS: The numerous combinations between different glass fillers are not able to completely satisfy all the requests of a dental restorative material. Our results suggest that the elaboration of a new dental material must first of all clarify the properties that we want to obtain. Thus for the restorations where esthetics is a priority in the anterior teeth we will use more translucent composite resins to match with the high translucency to the enamel; for the restorations in the posterior teeth where the resin must match the dentine we will use more opaque materials. The different values for the investigated composite resins are able to cover all the clinical applications of these materials.

**REFERENCES:** <sup>1</sup>Akerboom H.B., Kreulen CM., (1993), *J Prosthet Dent*, Oct, **70:**351. <sup>2</sup>F.Lutz, R.Phillips, (1984), *J. Dent. Res.*, **63:**914.

<sup>13</sup> Emil Isac Street, 400023 Cluj-Napoca, Romania <sup>2</sup> Dept. of Restorative Dentistry, University of Medicine and Pharmacy "Iuliu Hatieganu", 13 Emil Isac

Street, 400023 Cluj-Napoca, Romania

<sup>3</sup> Dept. of Dental Materials, "Raluca Ripan" Chemistry Research Institute, 30 Fantanele, Cluj-Napoca, Romania

### Silk as a biomaterial for controlled drug delivery

S. Hofmann<sup>1</sup>, C.W. Foo<sup>2</sup>, F. Rossetti<sup>3</sup>, M. Textor<sup>3</sup>, H.P. Merkle<sup>1</sup>, D.L. Kaplan<sup>2</sup>, L. Meinel<sup>1,2,4</sup>

<sup>1</sup> Galenische Pharmazie, ETH Zurich, Wolfgang Pauli Str. 10, CH-8093 Zurich,

<sup>2</sup> Department of Biomedical Engineering, Tufts University, Medford, MA 02155

<sup>3</sup> Oberflächentechnik, ETH Zurich, Wolfgang Pauli Str.10, CH-8093 Zurich,

<sup>4</sup> Division of Health Sciences and Technology, M.I.T, Cambridge, MA 02139

**INTRODUCTION:** The unique mechanical properties of silks together with their excellent biocompatibility have recently sparked interest of this protein polymer class for medical applications. This study details the possibilities and limitations for silk-based biomaterials as carriers for controlled drug delivery.

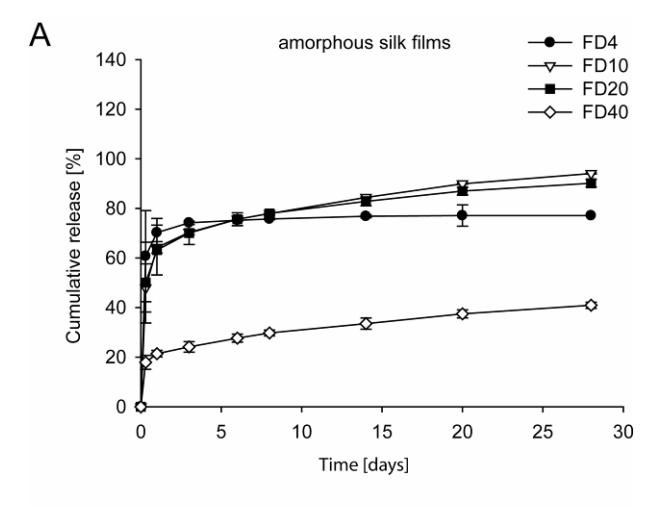
**METHODS:** FITC-Dextrans (FD) molecular weights of 4, 10, 20 and 40 kDa, and the proteins horseradish peroxidase (HRP) and lysozyme (LYS) were formulated into aqueous silk fibroin (SF). Dried films were treated with 90% (v/v) methanol (increasing crystalline SF structures) or H<sub>2</sub>O (referred to as amorphous silk). Release was quantified using HPLC (FD), colorimetric (HRP) and turbidimetric (LYS) methods. Conformational changes of SF were determined using FTIR and XRD, and crystalline/amorphous structures visualized by atomic force microscopy after with protease digestion.

**RESULTS:** Drug release from amorphous SF carriers was characterized by an initial burst exceeding 50% of total loading for all FD except for FD40. No substantial release was observed at later time points for the FD4 whereas the FDs with higher molecular weights were continuously released over the entire observation period of 30 days. With higher SF crystallinities, the initial burst was markedly reduced - for all FDs except FD4 - and a sustained release profile was ob-served for all FDs, particularly FD20 (**Figure 1**).

Protein release was tested with HRP and LYS, physically entrapped into the films. Using amorphous films, the release for both proteins was similar with an initial burst of less than 10 or 30 % for HRP and LYS, respectively. The initial burst was followed by a phase of low drug release from days 2 and 3, followed by a linear release until day 9. For crystalline films different release profiles were detected, characterized by an absence of a burst release and a continuous release of HRP starting at day 5 and no release for LYS over 30 days.

**DISCUSSION & CONCLUSIONS:** Drug release from SF films was a function of SF

crystallinity, drug size, and molecular structure. This data demonstrate interesting possibilities for the release of larger drugs (10 kDa or more) or proteins from SF films. Further studies are needed to detail release patterns for non proteinous low molecular weight drugs. **Together** with SF's interesting and distinguishing biomechanical features implant materials, our findings suggest a further avenue for the biomedical use of silks as both, implant materials and drug carriers.



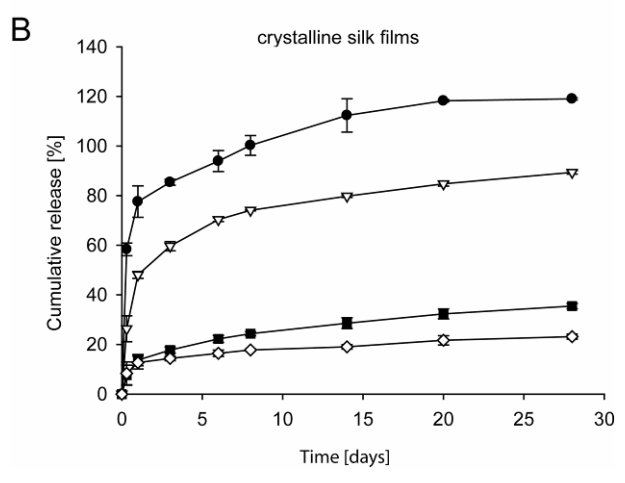


Fig. 1: Release of different FITC-dextrans from amorphous (A) or crystalline silk films (B).

**ACKNOWLEDGEMENTS:** We thank Trudel Ltd. (Zurich) for supply with silk cocoons, ETH Zurich (TH Gesuch), and the US National Science Foundation (# 0436490) for financial support.

### Weldability Study on Biocompatibile Co-Cr-Mo Alloys for Removable Partial Dentures using a Pulsed Laser

<sup>1</sup>Liliana Sandu, <sup>2</sup>Valentin Bîrdeanu, <sup>1</sup>Cristina Borţun

<sup>1</sup> "Victor Babeş" University of Medicine and Pharmacy, University Dental College, Spl. T. Vladimirescu nr. 14, Timişoara, România <sup>2</sup>National R&D Institute for Welding and Material Testing,Bd. Mihai Viteazul 30, Timişoara, România

**INTRODUCTION:** Pulsed laser welding is used in dental technology for more than ten years and it is applicable also in the area of removable partial dentures. The aim of the study was to determine the adequate parameters for the pulsed laser welding of Co-Cr-Mo alloys used in this field [1,2,3].

**METHODS:** For the preliminary trials, rectangular plates of different thiknesses (0,4 - 1 mm) were casted from the Co-Cr-Mo alloy (Vaskut Kohászati KFT), using classic procedures. This plates were welded in butt joint configuration, without filler material. For welding it was used a Nd:YAG pulsed laser HL 124P LCU (TRUMPF) (fig. 1), with the characteristics: peak power: 5kW; average power: 120W; pulse duration: 0,3-20 ms, max. repetition rate: 600 Hz; pulse energy 0,1-50 J.



Fig. 1. Laser HL 124P LCU (TRUMPF).

For the preliminary trials the peak power and the pulse duration were varied and the repetition rate was maintained at 1 Hz to assure a constant movement and a laser spot overlapping at 80-90%. The diameter of the spot varied between 0,5 and 0,6 mm. As protection gas was used Ar 99%.

### **RESULTS & DISCUSSIONS:**

After the preliminary trials the parameters of welding were established for the plates with thicknesses between 0,4 and 0,8 mm (Table nr. 1). For the 1 mm thick plates the weld cracked because the heat dissipated very fast in the material and the welded area cooled also quickly. For

thicknesses of 1 mm and more the experiments will be continued to establish the welding parameters.

*Table 1: Parameters of welding for the samples.* 

tuete 1. 1 di directe s of Westitting for the samples.				
sample	1	2	3	
peak power [W]	700			
pulse duration [ms]	20			
repetition rate [Hz]	1			
pulse energy [J]	14			
spot diameter [mm]	0.5	0.6	0.5	
spot overlap [%]	80-90			
speed [mm/s]	0.1	0.12	0.1	

The macroscopic aspects of the samples and the corresponding radiographies are shown in figure 2.

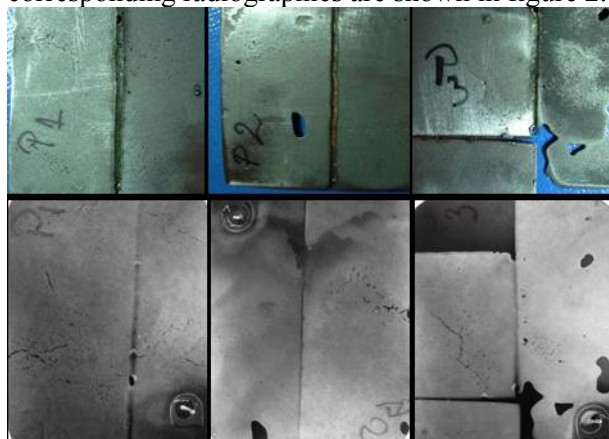


Fig. 2. Macroscopic aspects of the welded plates and the corresponding radiographies.

### **CONCLUSIONS:**

- The laser welding quality can be improved through variation of some laser parameters.
- Welding parameters were established of thin Co-Cr-Mo alloy plates.

REFERENCES: Lindemann W. (2000) Material-kundliche Untersuchungen an Laserschweiß-verbindungen zwischen Edelmetall- und Nichtedelmetalllegierungen, dental/labor, XLVIII, H2, pg. 199-202. Lindemann W. (2004) Plasma versus Laser, dental/labor, LII, H5, pg. 793-799. Schneidenbanger T. (2000) Der Einsatz des Lasers am Beispiel eines Klammerbruchs, dental/labor, XLVIII, H2, pg. 207-209.

### The effect of surface topography on human bone marrow cells

F.Baumgartner<sup>1</sup>, K.Maniura<sup>1</sup>, S.Tosatti<sup>2</sup>, M.Textor<sup>2</sup>, A.Bruinink<sup>1</sup>

<sup>1</sup> MaTisMed, Lab for Biocompatible Materials, Materials Science and Technology (Empa),

St. Gallen, Switzerland.

**INTRODUCTION:** Bone marrow cells contain among others mesenchymal stem cells that have the potential of self-renewal and can differentiate into various cell types such as osteoblasts, chondrocytes, myoblasts, fibroblasts and adipocytes [1]. These cells are among the first cells contacting the bone implant surface. This study investigates the effect of different defined surface topographies on the adhesion, morphology, migration and differentiation of these cells.

### **METHODS:**

The structured culture dishes were produced by injection moulding. Copies of the following topographies were fabricated; plane, a surface with hemispheres of 30  $\mu$ m in diameter and a spacing of 20  $\mu$ m (30/20), a surface with hemispheres of 50  $\mu$ m and no spacing (50/00), a polished and etched surface (p/e) and a surface with hemispheres of 30  $\mu$ m and 20  $\mu$ m spacing with a additional secondary etched structure (30/20e). The resulted dishes were titanium coated (70 nm) by physical vapour deposition, respectively sputtering.

Adult human bone marrow cells (HBMCs) were independently isolated from marrow of 3 patients obtaining a total hip replacement surgery. Adherent and expanded cells of the first passage were seeded out at a density of 5000/cm² and analysed after 7 days of cultivation. The cell viability was assessed by measuring the conversion of MTT to MTT-formazan per DNA as an index. Adherent cells were fluorescently stained for filamentous actin, the focal adhesion protein vinculin and the nucleus in order to enable a statement on the cytoskeleton architecture.

RESULTS: HBMCs on the 50/00 structure showed high MTT conversion per DNA values in comparison to all other structures whereas for p/e very low values were measured (Fig.1A) and was confirmed by another cell viability test (lysosomal activity, data not shown). CLSM analysis of the cultures showed variable cell densities and morphologies on the different structures (Fig.1B). On 50/00 surfaces the cultures were as dense as on the reference plane surface, whereas on all the other surfaces less cells were observed. On the 50/00 the cells span from one hemisphere to the other in contrast to the 30/20 where the cells were

located around the hemispheres. On both etched surface copies (p/e and 30/20e) the cells often formed star-shaped clusters.

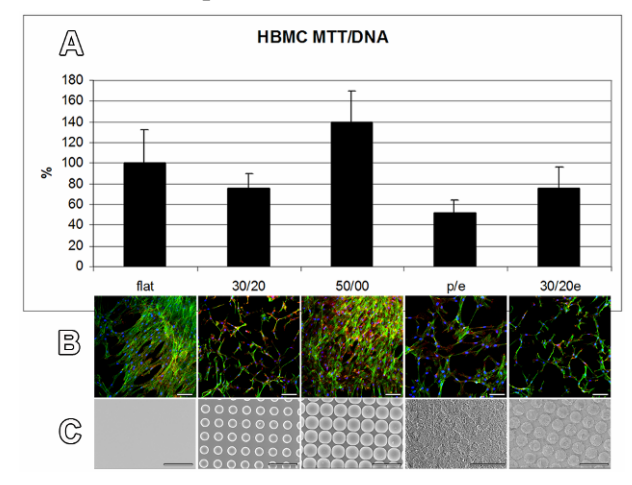


Fig. 1: HBMCs on different surface topographies. (A) MTT conversion per DNA, (B), HBMCs stained for F-actin (green), vinculin (red) and nucleus (blue), (C) raster electron microscopy images of the different topographies. Bar: 100 µm.

**DISCUSSION & CONCLUSIONS:** These results show that the topography influences the cell function and morphology. The 50/00 structure seems to promote cell adhesion, proliferation and has a positive impact on the metabolism of the cell. Furthermore, it can be assumed that HBMCs on copies of both etched surfaces behave differently from those kept on the polished 50/00. The comparison of the 50/00 with the 30/20 suggests that not the hemispheres itselves are the stimulating parameter, but rather the spacing between the hemispheres. The results of this study show how surface topography influences the functionality of the cells. Further investigations will be dedicated to the characterisation of the differentiation behaviour of HBMCs as function of surface topography.

**REFERENCES:** <sup>1</sup> Pittenger M.F. et al. (1999). *Multilineage potential of adult human mesenchymal stem cells, Science 284, 143-147.* 

<sup>&</sup>lt;sup>2</sup> Laboratory for Surface Science and Technology, Swiss Federal Institute of Technology (ETH), Zurich, Switzerland.

# DESIGN OF SURFACE-MODIFIED LIPID NANOSTRUCTURES FOR ORAL CALCITONIN DELIVERY

M. Garcia-Fuentes<sup>1,2</sup>, C. Prego<sup>1</sup>, D. Torres<sup>1</sup> and M. J. Alonso<sup>1</sup>

<sup>1</sup>Dept. of Pharmaceutical Technology, University of Santiago de Compostela, Spain. <sup>2</sup>Present address: Institute of Pharmaceutical Sciences, ETH Zurich, Switzerland.

**INTRODUCTION:** The use of submicrometric carriers has been proposed as a promising approach for overcoming the biopharmaceutical limitations that prevent peptide therapeutics from being successfully administrated by the oral route<sup>1</sup>. This experimental work was aimed at studying the influence of surface characteristics of new lipid-based colloidal carriers on their efficacy as peptide delivery systems<sup>2</sup>. Concretely, we have designed two new nanocarrier systems consisting of a solid lipid core (tripalmitin) and a hydrophilic coating, either (poly (ethylene glycol) (PEG) or chitosan (CS) for the oral delivery of salmon calcitonin (sCT).

METHODS: Lipid nanoparticles were prepared by a double-emulsion solvent evaporation technique as described elsewhere<sup>3</sup>. The PEG coating was achieved by the adsorption onto the lipid cores of the modified amphiphile PEGstearate. On the other hand, CS-coated nanoparticles were formed by means of the ionic interaction between the polycationic CS and the polyanionic surface of the lipid particles. The granulometry of the resulting systems were characterized by photon correlation spectroscopy, and the nanostructure of the carriers, including the composition and disposition of the surface molecules was characterized by electron microscopy, laser doppler anemometry and liquidstate NMR. The behaviour of the prepared systems was investigated "in vitro" following incubation simulated gastrointestinal fluids enzymes. Moreover, the ability of nanoparticle carriers enhance the permeability of hydrophilic molecules through the intestinal epithelium was tested in the Caco-2 cell line. Finally, these carriers were loaded with sCT and their capacity to encapsulate and release this peptide was studied. These loaded formulations were then administered to rats to check the capacity of these carries to enhance the pharmacological response to the peptide "in vivo".

**RESULTS:** The physicochemical characterization data evidenced the effective surface modification of these nanocarriers either with PEG or CS. Both carriers showed a great capacity to associate the model peptide salmon calcitonin. The nanosystems

developed were acceptably stable in gastrointestinal fluids and able to interact with Caco-2 cell monolayers irrespective of the coating composition. However, only those coated with CS showed permeation enhancing properties when applied in high concentrations to the Caco-2 cell monolayer. Finally, the results from the "in vivo" experiment indicated that CS-coated systems were very efficient at increasing the systemic absorption of salmon calcitonin, as revealed by the significant decrease in the serum calcium levels, whereas those coated with PEG resulted ineffective (Fig. 2).

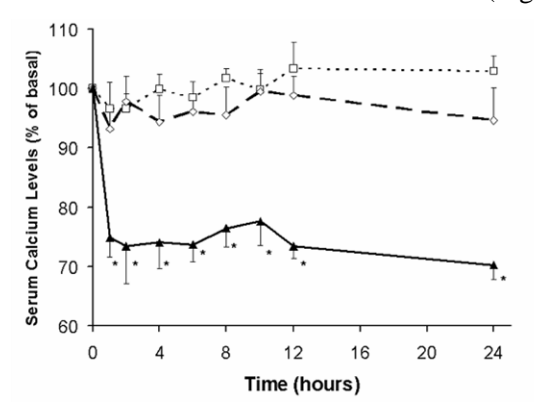


Fig. 2: Serum calcium levels (% of basal) in rats after administration of 500 UI/kg of ( $\square$ ) sCT in solution, ( $\Diamond$ ) sCT in PEG-coated nanoparticles and ( $\blacktriangle$ ) sCT in CS-coated nanoparticles (Mean  $\pm$ SD, n=6). \*Significantly different ( $\alpha$ <0.01).

**DISCUSSION & CONCLUSIONS:** Surface characteristics have shown to play a key role on the interactions of nanoparticles with the fluids and mucosal surfaces of the gastrointestinal tract. Altogether, these results suggest that CS surface-modified nanoparticles have a promising future for the oral delivery of peptide drugs.

**REFERENCES:** <sup>1</sup> A. T. Florence and N. Hussain (2001) *Adv Drug Deliv Rev* **50** (Suppl.1):S69-S89. <sup>2</sup> C. Prego, M. García, D. Torres and M. J. Alonso (2004) *J Control Release* **101**: 151-162. <sup>3</sup> M. Garcia-Fuentes, D. Torres, and M. J. Alonso (2002) *Colloid Surf B: Biointer.* **27**:159-168.

**ACKNOWLEDGEMENTS:** This work was financed by the Spanish Ministry of Science and Almirall Prodesfarma S.A.

### **Non-Destructive Defectoscopic Tests On Laser Welding Points**

### **In Partial Denture Alloys**

L. Ardelean<sup>1</sup>, C. Bortun<sup>1</sup>, L. Sandu<sup>1</sup>

 $^1$  "Victor Babes" University of Medicine and Pharmacy, University Dental College ,

2, Eftimie Murgu Square, 300041 Timisoara, Romania

**INTRODUCTION:** The quality of welding can also be tested by non-invasive methods, which make possible its macro- and microscopic assessment. This offers the possibility of assessing any defects in the structure of the alloy: in the welded area, in the thermal influence area or in the base material.

**METHODS:** The object of the study was the C alloy, produced by the Hungarian firm Vaskut Kohàszati Kft, which is currently used by us in making metallic components of partial dentures. Plates of a Cr-Co-Mo alloy were cast, their thickness varying from 0.4 mm to 0.9 mm, and they were welded with the laboratory Nd-Yag laser: LASER 65 L – TITEC.



Fig.1: LASER 65 L - TITEC with welding parameters

The studied areas were analyzed by non-destructive methods: basic fuchsin dye-staining, dental X-rays subsequently processed by computer pseudo-chromatization.

**RESULTS:** The welding area, with added materials (Co-Cr wire), dyed in yellow, shows the laser pulse sequences. No fissures are present in the immediate vicinity of the welding – in the thermal influence area – because the laser is used at very low temperatures and there are no contractions in the analyzed material. However, the X-rays show radio-transparence in the fusion area,

which indicates that the fusion is a superficial one and does not cover the entire thickness of the fused alloy. Although "C" material plates are not very thick, welding does not cover the whole depth. This results in the fragility of the welding.

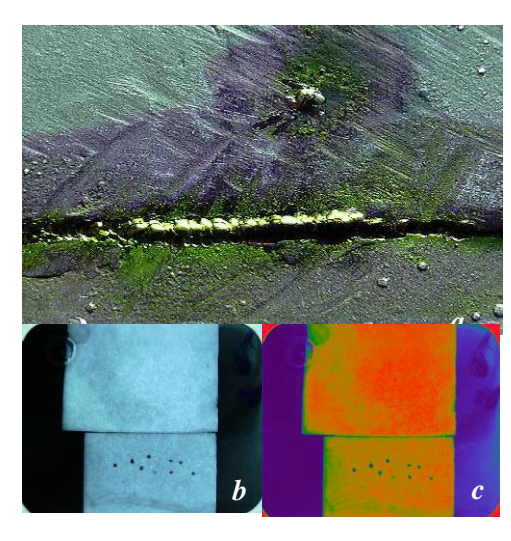


Fig.2: Assessment of the welded area: a. basic fuchsin dye-staining; b. X-ray; c. pseudo-chromatization.

**DISCUSSION & CONCLUSIONS:** The data in literature mention similar alloys used in dental technique [1-3], but they do not mention C alloy. The main advantage of the method is that of cold welding, even on a model. Plate assessment shows that the fusion area - laser welding - seems microscopically fragile, being easily breakable. X-rays do not show fissures in the fusion area or in the thickness of the basic material.

**REFERENCES:** <sup>1</sup>W. Lindemann (2000) *Dental/Labor* **XLVIII**: 199-202. <sup>2</sup>K. Päßler, B. Hottinger (1997) *Quintessenz Zahntech.* **23**: 909-919. <sup>3</sup>T. Schneidenbanger (2000) *Dental/Labor* **XLVIII**: 207-209

### **Etching Particle Assembly Systems: Producing Ordered Nanochemical Patterns**

T.M. Blättler, M. Textor, J. Vörös

Laboratory for Surface Science and Technology, BioInterfaceGroup, ETH Zurich, Switzerland

**INTRODUCTION:** Nanopatterns bioapplications are increasingly popular because they provide novel tools to address biological problems. For example, protein nanoarrays not only enable molecular level statistics of binding events but also offer an increased sensitivity compared to microarrays. Additionally, nanopatterning plays a key role in cell studies, where cell-cell or cell-extracellular matrix interactions can be investigated. Particles arranged into 2D ordered structures can serve as a template for the fabrication of well-defined nanostructures. Certain novel applications, such as single molecule fluorescence studies, require nano-sized features in geometrically ordered patterns with a separation between the features in the low micrometer range in order to be able to detect individual nanostructures by optical microscopy.

METHODS: To achieve such patterns we have self-assembled micron sized latex particles by controlled drying or spin coating in aqueous suspensions on silicon wafers and microscopy glass slides (sputter-)coated with 70 nm SiO<sub>2</sub> (intermediate layer) and 11 nm TiO<sub>2</sub> (overlayer). The latex particle patterns were then etched by reactive ion etching (RIE) to homogeneously reduce the size of the latex. Size and morphology of the latex features created after RIE strongly depend on the parameters, such as gas composition, forward power and chamber pressure, used during the RIE. The etched latex particle patterns can be used to create biologically active molecular assembly patterns by lift-off (MAPL) [1] or can serve as a mask to create an oxide contrast in the underlying substrate by RIE. The latter technique produces TiO<sub>2</sub> pillars in a SiO<sub>2</sub> background. With the selective molecularassembly patterning (SMAP) [2] technique the oxide contrast is translated into a biochemical contrast, by two simple dip-and-rinse processes. In short; alkane phosphates SAMs are created on the TiO<sub>2</sub> pillars by selective assembly and in a second step the SiO<sub>2</sub> background is passivated towards unspecific protein adsorption with poly(L-lysine)graft-poly(ethylene glycol) (PLL-g-PEG). SMAP patterns are then used for specific protein adsorption on the protein adhesive alkane phosphate SAM nanofeatures while background is protein resistant.

**RESULTS:** We will present results on SMAP nanopatterns as described above showing the

crucial steps and parameters starting from the selforganized latex particle patterns to the RIE patterns all the way to the nano-sized protein patterns produced by the SMAP technique.

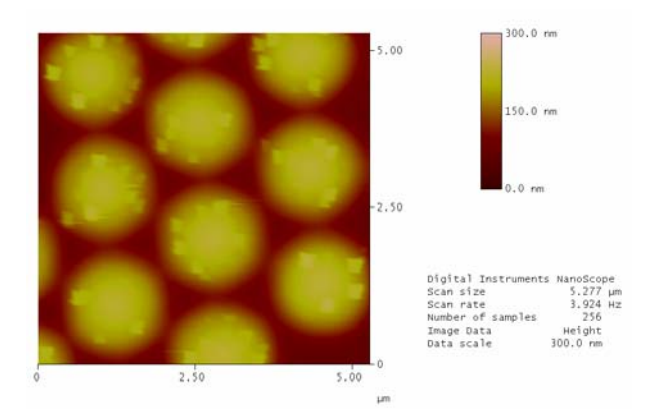


Fig. 1: AFM image of the etched oxide substrate after lift-off of the latex particles (1.9  $\mu$ m). The height of the pillars is ~110 nm. The pillars have a wavelike shape when looking at them in cross-section.

**DISCUSSION & CONCLUSIONS:** We were able to produce nano-sized features of  $TiO_2$  separated in the micron-range in a  $SiO_2$  background and could successfully apply these patterns to SMAP patterns.

Future applications of our nanopatterned substrates include the study of cell-surface, vesicle/bilayer as well as protein-surface interactions.

**REFERENCES:** <sup>1</sup>D. Falconnet, A. Koenig, F. Assi and M. Textor (2004) *Adv. Funct. Mat.* **14** (8): 749-756. <sup>2</sup>R. Michel, J.W. Lussi, G. Csucs, I. Reviakine, G. Danuser, B. Ketterer, J.A. Hubbell, M. Textor and N.D. Spencer (2000) *Langmuir* **18**:3281-3287.

ACKNOWLEDGEMENTS: This work, as part of the European Science Foundation EUROCORES Programme NanoSMAP, was supported by funds from the Swiss National Science Foundation (SNF) and the EC Sixth Framework Programme.

Many thanks to Christoph Huwiler and Marc Dusseiller for their help with the SEM and to Otte Homan from the Micro/Nanofabrication Lab (FIRST) at ETH-Hoenggerberg, Zurich.

### Properties of an injectable low modulus PMMA bone cement for vertebroplasty

A.Boger<sup>1</sup>, S.Verrier<sup>1</sup>, M.Bohner<sup>2</sup>, P.Heini<sup>3</sup>, E.Schneider<sup>1</sup>

<sup>1</sup> AO Research Institute, Davos, Switzerland. <sup>2</sup> Robert Mathys Foundation, Bettlach, Switzerland. <sup>3</sup> Orthopaedic Surgery, Inselspital Bern, Switzerland.

**INTRODUCTION:** To date, poly(methyl methacrylate) (PMMA) is by far the most frequently used material for vertebroplasty. However, PMMA has – among others - inadequate mechanical properties. Due to its high stiffness, an increased fracture risk has been demonstrated for the adjacent vertebral bodies after reinforcement<sup>1</sup>. It seems reasonable to assume that the optimal mechanical properties of the PMMA should be close to 500 MPa (Young's modulus, YM) and 5MPa (Yield strength, YS) to strengthen the remaining trabeculae in osteoporosis<sup>2</sup>. generation of pores within the PMMA might be an ideal way to decrease its stiffness. The goal of this study was to investigate the properties of the modified **PMMA** cement on radioopacity, polymerization temperature and monomer release in comparison to PMMA bone cement (Vertecem, Synthes Inc.).

**METHODS:** Porous cements were prepared by mixing the fluid PMMA paste (CEM) with a viscous aqueous solution. An aqueous solution of sodium hyaluronate (HA) 2% w/w is used for this purpose. The composition ratios CEM:HA were 100:0, 85:15, 70:30, 70:35, 60:40, 55:45 & 50:50.

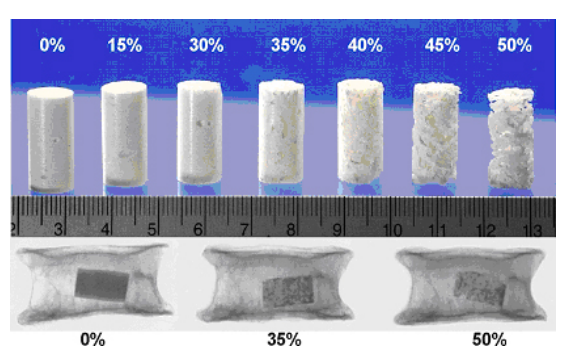


Figure 1: Optical (top) and radiological (bottom) aspects of porous PMMA cement samples. The aqueous fractions are given as percentage (HA).

Cylindrical samples (Fig.1 top) (length:20mm, diameter: 10mm, n=13 per group) were submitted to compression using a Instron 5866 (10kN load cell, 5mm/min speed). Young's modulus and yield strength were evaluated according to ISO 5833. Temperature during hardening was measured and the setting time was determinate (n=3 per group), using a Pt100 sensor (ISO 5833). The viscosity of the cement was estimated by measuring the force

needed to extrude the cement out of a 5ml syringe connected to a 150mm long 8 Ga needle (Instron 5866, n=9). Radioopacity of the cement was tested within a human lumbar vertebral body (L3, 70 years) using a fluoroscope (ARCO-SI 100, 50keV, 0.5mA). To measure the monomer release, 4mL of the freshly mixed cement were injected into a cotton bag, hanging in 3.51 Ringer lactate solution at  $37\pm3^{\circ}$ C. Fluid samples were taken at different time points during 14 days of leaching time and the amount of MMA was analysed by gas chromatography. The mechanical properties and viscosity results were statistically analysed using ANOVA and a non parametric T-test ( $\alpha$ =0.05).

**RESULTS:** Stiffness decreased from  $1.9 \pm 0.03$ GPa to  $0.12\pm 0.045$ GPa and yield strength decreased from  $100\pm 5$ MPa to  $2.6\pm 1.1$ MPa, when the aqueous fraction was increased from 0 to 50%. The maximum temperature decreased from  $70 \pm 3.5$  °C (after  $18 \pm 2$  min setting) for Vertecem cement to  $40 \pm 1$ °C (after  $10\pm 1$ min setting) for 45% porosity. Beside an adequate viscosity around 100Pa\*s before hardening -of the porous materials, the different materials have also adequate radio-opacity until an aqueous fraction of 40% (Fig.1 bottom). The maximum amount of released MMA was around 6.3, 4.5 and 7.2 mg MMA / ml cement volume for the 100:0, 70:30 and 55:45 materials compositions, respectively.

**CONCLUSIONS:** Generation of pores in bone cement is a promising solution to soften PMMA: addition of aqueous fraction of around 35% was able to reach the mechanical properties of around 500MPa in stiffness. Adjustment of the mechanical properties of PMMA is expected to reduce the fracture risk of adjacent vertebral bodies.

**REFERENCES:** <sup>1</sup> Grados et al (2000) *Rheumatology*, <sup>2</sup> Banse et al (2002) *J.Bone & Mineral Research.* 

**ACKNOWLEDGEMENTS:** The authors thank Synthes Biomaterials for providing the Vertecem cement.

**CONTACT:** andreas.boger@aofoundation.org

### Synthesis and characterization of porous beta-tricalcium phosphate blocks

M. Bohner<sup>1</sup>, G. H. van Lenthe<sup>2</sup>, S. Grünenfelder<sup>1</sup>, W. Hirsiger<sup>1</sup>, R. Evison<sup>2</sup>, R. Müller<sup>2</sup>

<sup>1</sup> Dr h.c. Robert Mathys Foundation, Bettlach, Switzerland. <sup>2</sup> ETHZ and University of Zürich, Zürich, Switzerland.

**INTRODUCTION:** Porous beta-tricalcium phosphate (b-TCP) blocks with four different pore sizes were synthesized using "calcium phosphate emulsions", and characterized by optical, physical and radiological methods. The goal of this communication is to present the synthesis, the characterization methods, and the results.

**METHODS:** 80g b-TCP and 20g TCP were added to 100g viscous paraffin oil and 67mL of an emulsifier solution. These compounds were stirred at 2000 RPM, poured into 8 moulds, incubated for 24 hours until complete hardening occurred, cleaned with petroleum ether, dried and sintered at 1250°C to obtain phase-pure -TCP. Finally, the samples were machined to obtain small cylinders (8x13mm).

The geometry of the cylinders was characterized by calculating their macroporosity based on their composition, by measuring their apparent density, and by determining their average pore size based on optical photos of the block surface. The samples were also observed by scanning electron microscopy and micro-computed tomography (mCT).

**RESULTS:** The reproducibility of the synthesis method was very good. The microporosity, macroporosity and the total block porosity were close to 21%, 54% and 75%. The macropore diameter was close to 150, 250, 500 and 1200 um, as measured optically. Slightly lower values were obtained by mCT. The mCT macroporosity was 53-54%. A very good linear correlation was found between the mCT and optical pore size, as well as between the radio-density and the apparent density.

**DISCUSSION & CONCLUSIONS:** These results suggest that optical, physical and radiological methods can be combined to characterize the geometry of ceramic blocks.

### Nanocomposite used in dentistry

A.Colceriu<sup>1\*</sup>, M.Moldovan<sup>1</sup>, C.Prejmerean<sup>1</sup>, T. Buruiana<sup>2</sup>, E.C. Buruiana<sup>2</sup>, G.Furtos<sup>1</sup>, L.Vezsenyi<sup>1</sup>, D. Prodan<sup>1</sup>& C.Tamas<sup>1</sup>

<sup>1</sup> "Raluca Ripan" Chemistry Research Institute, Cluj-Napoca, Romania

<sup>2</sup> "Petru Poni" Institute of Macromolecular Chemistry, Iasi, Romania

**INTRODUCTION:** Nanocomposites are the premises of new materials that can be applied in many fields due to their improved mechanical properties (determined by the reinforcement of nanoparticles in the organic part), to their lightweight, and to their light conducting properties. The purpose of this study is to *obtain and characterize some inorganic fillers and* some new urethane diacrylates; and also to study the flexural strength (FS), the compressive strength (CS), the diametrical tensile strength (DTS), of the three nanocomposites.

**MATERIALS AND METHODS:** The organic phase consists of (75-45)% some urethane diacrylates including hydrophilic urethane diacrylate oligomers: CH<sub>2</sub>=C(CH<sub>3</sub>)-(CH<sub>2</sub>)<sub>2</sub>-OCOHN-**R**-NHCOO-[(CH<sub>2</sub>)<sub>2</sub>O]<sub>n</sub>-CONH-**R**-

NHCOO-(CH<sub>2</sub>)<sub>2</sub>-C(CH<sub>3</sub>)=CH<sub>2</sub> (R-is rest of isophorone disocyanate), dimetacrilate monomers TEDMA; CQ, DMAEM, and BHT as polymerization inhibitor. The compositions of the organic phase are shown in table 1.

Table 1. The organic phase [wt%]

Table1. The Organic phase [wi/0]						
Liquid	Urethane diacrylates	%	TEDMA			
L1	IFDI+HEMA(izophorone diizocynate	75	25			
	+ 2-hidroxyetylmetacrilate); M1					
L2	IFDI+PEG(300)+HEMA; M2	43	57			
L3	PEG(1000)+HMDI+HEMA; M3	46	54			

The nanocomposites were prepared as a paste, by dispersing the synthesized nanoparticles (Al<sub>2</sub>O<sub>3</sub>-ZrO<sub>2</sub>) and glasses (glass with Ba) in the monomer mixture. Nanoparticles obtained by sol-gel method and glasses was silanizated with 3-methacry loyloxypropyl-1-trimethoxy-silane (silane A-174). The compositions of the light-curing nanocomposites are shown in table 2.

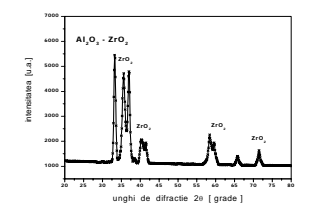
Table 2. The nanocomposites [wt%]

Cod nanocom	Organic phase	Inorganic Phase			
posite	phase	$\begin{array}{c c} (Al_2O_3\text{-}&Glasses\\ ZrO_2);&N_1&G_1 \end{array}$		SiO <sub>2</sub> colloidal	
C1	L1-18	25	50	25	
C2	L2-19	30	55	15	
C3	L3-21	35	50	15	

We followed by IR spectroscopy the reaction by which urethane diacrylates were formed, and we mainly monitored the disappearance of the 2125 cm<sup>-1</sup> band that characterizes the isocyanogen group. *Characterization of the nanoparticles* was made by *X-ray diffraction*. The **X** – **ray** scattering patterns were obtained by means of standard DRON-3M powder diffractometer, working at 40 kV and 30 mA The CuKa (l=1.54178 Å) radiation, Ni filtered, was collimated with Soller slits. *Characterization of the nanocomposites*. The tests for the mechanical properties (CS, FS, DTS) were made on a universal mechanic testing instrument,

INSTRONE brand of the VEB Thürignger Industrie Werk Rauenstein Company.

**RESULTS:** X-ray diffraction patterns (Fig. 1) evidence the crystalline phases  $(N_1)$  developed in these samples. The main diffraction maximum points for the G1 compound are very wide, characteristic to an amorphous system.



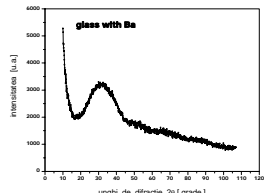


Fig. 1: DRX patterns for  $N_1$  and  $G_1$  samples The diffractogram shows the main maximum points for ZrO<sub>2</sub> – Powder Diffraction File (PDF) 7-337, the cubical system (fig.1), and also the main aluminum oxide-based crystalline components. In the IR spectres of the M<sub>1</sub>, M<sub>2</sub> and M<sub>3</sub> monomers, we can notice bands that are specific to existing groups in each compound's structure. Thus, the 3350 cm<sup>-1</sup> absorption bands are determined by the frequency of the dilation vibrations of NH urethane group, while the 2950 cm<sup>-1</sup> bands by the dilation vibrations of C-H and CH<sub>2</sub> from the structure of the acrylic urethane monomer. The results regarding FS tests show values between 70-85 MPa, the lowest value being issued by C3. Results for the CS show values between 280-260MPa, the lowest value being for the C3 composite. The values obtained for the DTS are between 35-40 MPa.

**DISCUSSION & CONCLUSIONS:** The results show that  $N_1$  and G1 samples own filler properties that recommend them for dental composites materials. Often the mean particle filler size is given in an attempt to characterize the type of material. The presence of the urethane structure (-NHCOO-) related to the peptide link (-NHCO-) is a recent development for the dental composites.

Observing the tests made on the composites obtained in our laboratory, it can be seen that the mechanical properties depend on the nature and the concentration of the inorganic filler.

### **REFERENCES:**

<sup>1</sup> S.L Wendt, K.F.Leinfelder (1994) *Am J Dent* **7**:207-211; <sup>2</sup>M.Chatterjee, M.K.Nasakar, D.Ganguli (2003) *J. of sol-gel Sci. and Tech.* **28**:217-225

Using mineral trioxide aggregate and calcium hydroxide as a pulp-capping materials

L.Colceriu<sup>1</sup>, S.Cimpean<sup>1</sup>, A.Pop<sup>1</sup>, M.Moldovan<sup>2</sup>, A.Colceriu<sup>2</sup>

<sup>1</sup> Department of Odontology and Periodontology, University of Dental Medecine"I.Hatieganu"

<sup>2</sup> "Raluca Ripan" Chemistry Research Institute, Cluj-Napoca, Romania

INTRODUCTION: Pulp capping is defined as the placement of a dental material over an exposed pulp to initiate the formation of irritation dentin at the site of injury. Classically, different formulations of calcium hydroxide (CH) have been used. Today, a newer material is advocated for vital pulp therapy, mineral trioxide aggregate (MTA). We proved that the exposed dental pulp has the capacity to heal when microleakage and bacterial contamination are prevented. Therefore, it appears that an effective pulp-capping material should be biocompatible, that it should provide a biological seal and prevent bacterial leakage.

METHODS: In this experiment we used 10 premolars upper and lower. We isolated the teeth with a rubber dam and, using a round bur in a high-speed handpiece with a copious water spray, we created standardized pulp exposures (1 millimeter in diameter) by a vestibular access opening. We controlled bleeding with sterile cotton pellets before placing the pulp-capping materials. The materials used were either a calcium hydroxide preparation or MTA. Eventually, we surgically removed the teeth and perfused them with formalin. The specimens were processed for histological examination. The sections were stained with hematoxylin and eosin.

**RESULTS:** The pulps capped with MTA or calcium hydroxide showed dentin bridge formation or dentin chips present. Dentin chips may promote or retard healing. A dentin bridge has formed a complete barrier at the exposure site and the pulp is free of inflammations. The reparative dentin did not originate from severely damaged odontoblasts; instead, undifferentiated cells that migrated from

deep regions of the pulp replaced the degenerated odontoblasts. This explains why the reparative dentin is regular when is formed from areas where the odontoblasts remain intact.

**DISCUSSION & CONCLUSIONS:** Based on the results of this study and the properties of materials we demonstrated that MTA and calcium hydroxide are suitable as pulp-capping materials during vital pulp therapy. The pulp-capping procedures used here resulted in the pulp being mechanically exposed. In future work pulp reaction to MTA and CH in carious pulp exposures should be tested.

### **REFERENCES:**

- <sup>1</sup> Ford P., Torabinejad M., *JADA* 1996; **127**:1491-1494.
- <sup>2</sup> Holland R., Valdir de Souza, Nery Mauro J., Filho J.A. Otoboni, Bernabe P.F.E., Dezan Eloi., *Journal of Endodontics* 1999; **25**:161-166.
- <sup>3</sup> Torabinejad M., Chivian N., *Journal of Endodontics* 1999; **25**:197-204
- <sup>4</sup> Fitzgerald M, Heys RJ. *Oper Dent* 2001; **16**:101-12
- <sup>5</sup> Baume LJ, Holz J. *Int dent J* 2001; **31** :251-60

# Cell viability and matrix synthesis of cancellous bone explants maintained *ex vivo* within the "Zetos" culture system.

CM. Davies <sup>1</sup>, PI. Jäggi <sup>1</sup>, CW. Archer <sup>2</sup>, DB. Jones <sup>3</sup> and RG. Richards <sup>1</sup>.

<sup>1</sup>AO Research Institute, Davos, Switzerland, <sup>2</sup>Cardiff School of Biosciences, Cardiff University, Wales (GB) <sup>3</sup>Experimental Orthopaedics & Biomechanics, Philipps University Marburg, Germany.

INTRODUCTION: The Zetos culture system<sup>[1]</sup> has potential to keep human cancellous bone tissue viable *ex vivo*<sup>[2]</sup> through the use of unique chambers and a loading device that allows the tissue to remain in its natural 3D milieu. The loading device allows the tissue to receive physiological mechanical loading which is not possible with most organ cultures. This loading is believed to increase cell viability. The aim of this study was: 1) to assess cell viability through the labelling of live and dead cells simultaneously and 2) to observe cell matrix synthesis by labelling active protein synthesis with tritiated glycine and *de novo* bone apposition through double fluorescent labelling.

**METHODS:** Cancellous bone explants 5 mm high and 10 mm in diameter were harvested from human femoral heads, distal ovine femora or distal bovine metacarpals<sup>[3]</sup>. Explants were loaded daily in the loading device for 300 cycles at 1Hz applying 4,000 ustrain. Cores were processed for histological and immunohistochemical evaluation<sup>[3]</sup>. 3H-glycine was placed in the media for 24 h allowing incorporation into newly synthesised proteins. Media and tissue proteins were harvested and analysed for radioactivity Fluorescent double labelling with calcein (green) and alizarin (red) was incorporated into growing tissue at day 1 and 11 respectively to assess de novo bone apposition.

**RESULTS:** <sup>3</sup>H-glycine was detected in protein through SDS-page analysis well as autoradiography embedded of sections. demonstrating cell viability after both 7 and 15 days culture (Fig.1a). Sequencing of proteins confirmed the protein to be collagen. Bone apposition was observed at the surface of explants (Fig.1b) supporting the assumption that the tissue viable and producing bone matrix. Histological sections showed fresh osteoid seams; bone and marrow cells were well preserved. Very little necrotic tissue was observed, though a ring of bone debris and fibrous-like encapsulation was observed at the core periphery. Noncollagenous proteins, and procollagen Type I were localised through immunohistochemical labelling of sections.

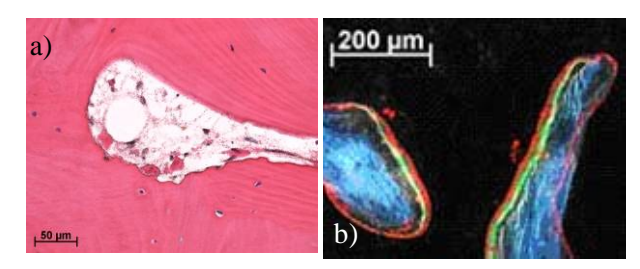


**Figure 1. a)** Autoradiograph of ovine tissue, cultured for 7 days within Zetos. Protein production observed in osteocyte lacunae. **b)** Bone apposition detected in 71 year old male explant, cultured for 15 days.

Loaded tissue demonstrated better viability than unloaded disuse controls. However, a diffusion limitation was observed with the cancellous bone cores, irrespective of culture method. It was also noted that the bathing of the cores cultured within the Zetos chambers were inferior to submerged static controls cultured within centrifuge tubes at this time period.

DISCUSSION & CONCLUSIONS: Culture of cancellous bone explants within the loaded Zetos system maintained bone cells viable and synthesising matrix for at least 15 days. Cells from loaded explants were qualitatively more active than unloaded explants, however the chamber design was observed to reduce the diffusion of the tissue in comparison to control explants. Modification of the chamber is required and determination of duration of viability in non-loaded centrifuge tubes will be undertaken. Further validation is ongoing with variation in core dimensions, media and evaluation of effects of growth factors.

**REFERENCES:** [1] Jones D.B. *et al.*, (2003). *Eur Cell Mater* **5**: 48-60 [2] Clarke M.C.H., *et al.*, (2003). *J. Cell Biol.* **160**:4 577-587. [3] Yang R. *et al.*, (2003) *Eur Cell Mater* **6**: 57-71.

**ACKNOWLEDGEMENTS:** Funded by the 3R Foundation grant # 78/01 and # 86/03. The authors wish to thank to Dr Thomas Perren for supplying human tissue.

### Antibacterial Behaviour of a Silver-Doped Glass for Bone Surgery

S. Di Nunzio<sup>1</sup>, M. Miola<sup>1</sup>, E. Vernè<sup>1</sup>, A. Massè<sup>2</sup>, G. Maina<sup>2</sup>, G. Fucale<sup>3</sup>

<sup>1</sup> Material Science and Chemical Engineering Dept. - Polytechnic of Turin, Turin, Italy.

**INTRODUCTION:** The prevention of infections disease represents nowadays a central need, especially for prosthetic surgery. Many nosocomial bacteria, in fact, show an increasing resistance towards antibiotics, causing serious infections that lead to prolonged times of hospitalisation. The development of surfaces with low bacterial adhesion together with biocompatibility can represent a solution to prevent infections. Biocompatible glasses can be used to realize bone substitutes as well as coated metallic devices; moreover such materials can be opportunely treated to enrich their surfaces with silver ions [1] thus providing a controlled ion release and consequently antibacterial efficacy. Silver is, in fact, a well-known broad-spectrum antimicrobial agent, so silver-doped glasses can be produced to realize different devices, such as bone substitutes or coated metallic implants, with antibacterial action.

**METHODS:** A biocompatible glass composition was selected, processed by ion-exchange treatment to introduce a controlled amount of silver ions on its surface and, finally, characterized in terms of silver release in simulated body fluid solution (GF-AAS) and antibacterial activity (*S. Aureus* and *E. Coli*). Release tests were performed analyzing SBF at increasing times of contact with silver doped glass samples. Antibacterial tests evaluated bacteria adhesion on silver containing samples surfaces compared with untreated glass and PE control by means of colony forming unit (CFU) counts; moreover also culture medium was examined after samples incubation.

**RESULTS:** GF-AAS tests results are graphically shown in *figure 1*: the maximum amount of released silver ions is below 2μg/cm²; release rate is higher for shorter times of SBF exposure to silver doped samples, reaching a threshold after about 500 hours. Antibacterial tests demonstrate, as evident in *figure 2* (only S. Aureus results are reported), that the introduced silver amount is sufficient to guarantee an antibacterial activity towards both *S. Aureus* and *E. Coli*.

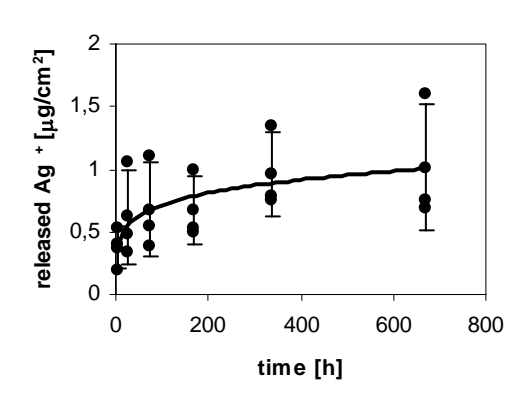


Fig. 1: GF-AAS measurements of silver ions released from doped glass samples into SBF solution.

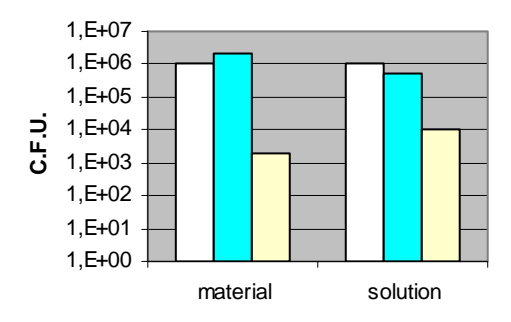


Fig. 2: C.F.U. counts after 24 hours incubation of S. Aureus on PE control (white bars), untreated glass (blue bars) and silver doped glass(yellow bars); both bacteria adhered on material surface and proliferated into culture medium were counted.

**DISCUSSION & CONCLUSIONS:** Release tests results are in accordance with literature data safe concentrations concerning Moreover the release rate trend shows that the stronger activity of silver is obtained immediately after contact with SBF solution; commonly, higher risks of infections occur immediately after surgical operations. Antibacterial tests demonstrates that silver doped glasses prepared by ion-exchange treatment are effective against S. Aureus and E. material surface adhesion onto proliferation in the surrounding culture medium: in both cases, in fact, C.F.U. decreased of at least 2 order of magnitude respect to control samples.

**REFERENCES:** <sup>1</sup> E. Vernè et al., *Surface characterization of silver-doped bioactive glass*, Biomaterials, **26**:25 (2005); pp. 5111-5119.

<sup>&</sup>lt;sup>2</sup> Traumatology, Orthopaedics and Occupational Medicine Dept. - University of Turin, Turin, Italy. <sup>3</sup> Chemical, Clinical and Microbiological Analyses Dept. of CTO, Turin, Italy

# The micro/nano proton beam as a tool for the Bio PIXE analysis of the in vivo biocompatibility of implants at the bone interface



G. Guibert, F. Munnik and S. Mikhaïlov CAFI, Centre d'Analyses par Faisceau Ionique, Le Locle

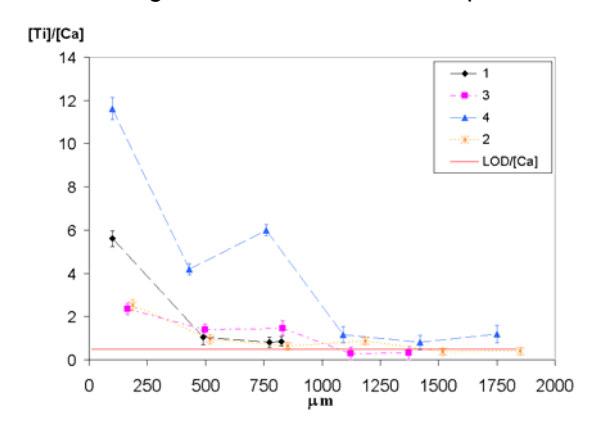


At CAFI, a micro/nano, high energy ion-beam tool has been installed in collaboration with Oxford Microbeams. With this facility, beams of light ions (protons, He ions) with an energy up to 3.5 MeV can be focussed to dimensions in the micrometer to nanometer range. In a first stage, we have achieved beam dimensions around 1  $\mu$ m but further improvement is foreseen and the state-of-the-art is 35×75 nm², achieved at Singapore University. In the standard configuration, the manipulation takes place in vacuum but an external microbeam has also been developed in which the ion beam passes through a thin window into air.

Many applications are possible with this versatile tool: it can be used for the maskless 3D structuring of photo-resist materials, for structured implantation and material modification and for 2D/3D analysis. The analysis can use techniques such as Particle Induced X-ray Emission (PIXE), Rutherford Backscattering Spectroscopy (RBS). The focussed high-energy ion beam is scanned over the sample with an area that is continuously variable from tens of a micrometer up to 2 mm to obtain 2 or 3 dimensional imaging of elemental distributions in a specimen. The field of application for analysis is vast, from Bio-medical and environmental research, Earth science, Art and archaeology, to materials science.

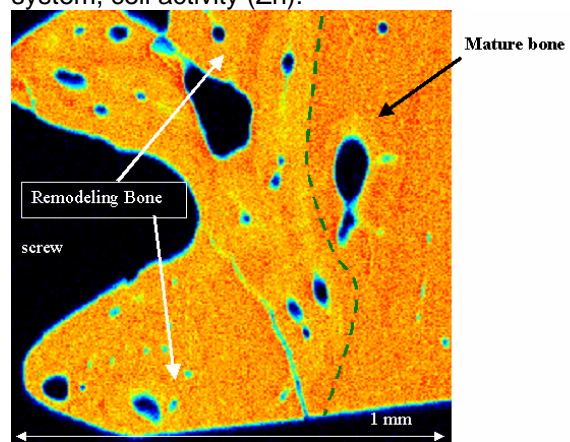
In this poster, we present the application of this micro/nano beam facility to the characterisation of sheep bone implanted with metal screws in order to see the effect of different surface treatments of the implants and their biocompatibility. Sheep were implanted with several types of screw. After the few months, the bones with the screws were removed and samples were prepared by cutting the bone, removing the screw, embedding the bone in epoxy resin and polishing. These samples have been analysed with PIXE and RBS in the micro/nano beam facility at CAFI to obtain elemental distribution maps and concentration profiles at the bone-implant interface. One result is presented below, others are presented in the poster.

Metallic migration: nature, content, depth:



Titanium migration from implant (coord. 0) towards bone. Sample 1, 2, 3, 4. [Ti] is normalized by [Ca]. LOD: Limit of detection.

Bone characterisation: remodelling, vascular system, cell activity (Zn):



Ca distribution near metal screw by PIXE. Bone near screw contains cavity, this area corresponds to remodeling bone.

### Conclusions:

[Ti] average concentration is similar for samples 1,2,3, except for 4, which is more polluted ( $\approx$  200  $\mu$ g/g). Titanium grains are observed near the implant and their size can reach 10  $\mu$ m. Grains can move into bone towards the vascular system.

New bone, coming from damaged bone remodelling, reaches several hundred  $\mu m$  thickness. A higher concentration of [Zn] in this region confirms this observation.

Great sensitivity, simultaneous multi-element analysis and micrometric resolution over a large area make microbeam PIXE a useful tool for biological and biomedical analysis.

This work is performed in the framework of the CTI project 5263.1HES

# Cytocompatibility of coated titanium surfaces impregnated with an antiseptic to staphylococci and fibroblasts

L.G. Harris<sup>1</sup>, L. Mead<sup>1</sup>, E. Müller-Oberlander<sup>2</sup>, R.G. Richards<sup>1</sup>

AO Research Institute, Davos, Switzerland

<sup>2</sup> Synthes Inc., Oberdorf, Switzerland

INTRODUCTION: Staphylococcus aureus and Staphylococcus epidermidis are both commonly associated with open fractures and external fixators. These bacteria account for 3-40% of reported cases<sup>1,2</sup>, can lead to osteomyelitis and septicaemia, and with the rise in antibiotic resistant bacteria are an important issue<sup>3</sup>. Once adhered, S. aureus and S. epidermidis form biofilms which can be difficult to clinically treat because the bacteria are protected from phagocytosis and antibiotics<sup>4</sup>, hence the need to prevent initial bacterial adhesion. This study describes the cytocompatibility of different coated with/without surfaces chlorhexidine diacetate (CHA) to S. aureus, S. epidermidis, and hTERT fibroblasts.

**MATERIALS AND METHODS:** To visualise S. aureus and S. epidermidis adherence on different surfaces (Poly-D,L-lactide (PDLLA), politerefate (PTF), anodic plasma chemical deposited calciumphosphate (CaP/APC), polyurethane (PU), and polyvinylpyrrolidone (PVP)), bacteria were cultured on the different surfaces in brain heart infusion broth (BHI) at 37°C for 2h, 24h, 48h and 96h, then fixed for visualisation with an scanning electron microscope (SEM). To quantify the amount of bacteria on the surfaces, adherent bacteria were detached by sonication in Tween 80, then stained with a live/dead assay, and then counted with a Partec PAS flow cytometer. The amount of bacteria in the media was also counted using the same procedure. To determine the cytocompatibility of the surfaces to hTERT fibroblasts, cells were cultured on the surfaces in DMEM with 10% FCS at 37°C for 48h, then fixed for the SEM and the amount of spreading analysed. The cumulative release kinetics of CHA from the coated surfaces was analysed, and the adhesive strength of the coating mechanically tested.

**RESULTS:** On the surfaces without CHA, both staphylococcal strains and spread fibroblasts were observed, but on the CHA impregnated surfaces few bacteria (Fig. 1) and no intact fibroblasts were seen (Fig. 2). Flow cytometry found fewer bacteria in the media and on the surfaces containing CHA in comparison to the surfaces without CHA (Fig. 3). The release kinetics varied from slow to burst release: PDLLA > PTF > PU > CaP/APC = PVP.

With the exception of PU and PVP, the other three coatings passed the mechanical testing.

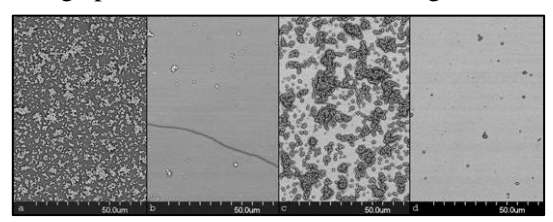


Fig. 1. SEM images of S. aureus (a-b) and S. epidermidis (c-d) on PU without CHA (a & c) and with CHA (b & d) after culturing for 48h.

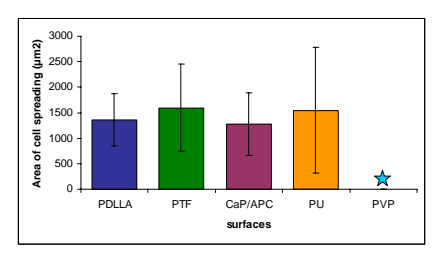


Fig. 2. Average spreading of hTERT fibroblasts on the different surfaces without CHA.. Star = little or no cell spreading so was not analysed.

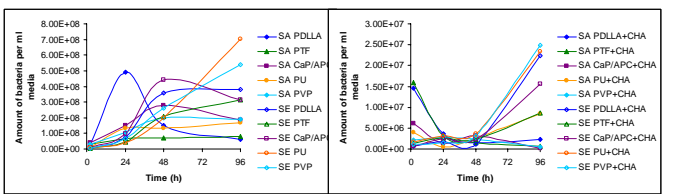


Fig. 3. Flow cytometer analysis of the media after culturing S. aureus (SA) and S. epidermidis (SE) for 2h, 24h, 48h and 96h on a) different surfaces without CHA, and b) with CHA.

**DISCUSSION & CONCLUSIONS:** This study showed that PDLLA and Politerefate (PTF) have potential as coatings for drug delivery, since they were cytocompatible to hTERT fibroblasts, eluted CHA effectively, and passed mechanical testing. However, since CHA was toxic to hTERT fibroblasts *in vitro*, the cytotoxicity of CHA needs further evaluation before it can be tested *in vivo*.

**REFERENCES:** <sup>1</sup>Lee-Smith J, Santy J, Davis P, Jester R, Kneale J (2001) J Orthop Nursing 5:37-42; <sup>2</sup>Khatod M, Botte MJ, Hoyt DB, Meyer RS, Smith JM, Akeson WH (2003) J Trauma 55:949-954; <sup>3</sup>Lowy FD (1998) New Eng J Med 339: 520-532; <sup>4</sup>Hoyle BD, Costerton JW (1991) Prog. Drug Res. 37:91-105.

**Acknowledgements:** Thanks to Benno Schmidhauser (Synthes Inc.), John Disegi (Synthes Inc.), Falko Schlottig (Synthes Inc.), Kati Gorna (ARI) and Vinz Frauchiger (RMS, Bettlach) for the various coatings.

### Electrolytic Deposition of Valve Metal Oxide Thin Films as Interference Coatings on Biomedical Implants

P. Kern, P. Schwaller, J. Michler

EMPA, Materials Technology Section, Thun, Switzerland

INTRODUCTION: Electrolytic deposition is an important, cost-effective tool in the formation of metallic, ceramic or organic films, including nanostructured materials and monolayers. Recently, great interest has emerged in electrolytic deposition of oxide films such as TiO2, Nb2O5 and ZrO<sub>2</sub> [1,2]. Such films are highly attractive for photovoltaic, electronic, electrochemical oxygen sensor (e.g. sensor) applications. Furthermore, the excellent biocompatibility and the thickness dependent interference color predefine these oxide films for biomedical applications, e.g. for color-coded biocompatible layers on nonanodizable biomedical alloys.

METHODS: Thin TiO<sub>2</sub>, Nb<sub>2</sub>O<sub>5</sub> and ZrO<sub>2</sub> films were electrolytically deposited on AISI 316L, Ti6Al4V and CoCrMo substrates via hydrolysis of peroxocomplexes by electrogenerated base using TiCl<sub>4</sub>, NbCl<sub>5</sub> and ZrOCl<sub>2</sub> salts in methanol/water mixtures. Deposition occurred statically at 0°C using a simple 2-electrode setup and a computercontrolled power source. Post-heat treatment of the as-deposited metal-peroxide films lead densification and cristallization. Film morphology and structure were analyzed by SEM, TEM and Raman. The chemical composition was assessed by quantitative depth profiling with glow discharge emission spectrometry (GD-OES). optical Nanoindentation and nanoscratch tests were performed using a MTS Nanoindentor XP with a Berkovich diamond tip.

**RESULTS:** Optimization of electrolyte formulation and deposition parameters lead to stoichiometric titania films with almost uniform thickness and hence. thickness-dependent interference colors, similar as known from the color-anodization process of Ti-alloys. Crack-free films were found up to 140 nm on AISI 316L and up to 190 nm on Ti6Al4V substrates. After thermal annealing at 450°C of as-deposited amorphous peroxotitanium hydrate films, Raman and TEM showed highly stoichiometric, nano-crystalline anatase films. GD-OES showed dehydration and densification during heat treatment and revealed stoichiometric TiO2 films on AISI 316 L with small Fe (3-4 at-%) and Cr (1 at-%) contamination due to thermal diffusion from the substrate. On the Ti6Al4V substrates, the comparison between

electrolytic TiO2 films and color-anodization in and phosphoric acid containing electrolytes showed significant higher purity of electrolytic films, absent of V, Al, S, P contaminations as found in anodic oxides (4-6 at-% Al, 1-2 at-% V). Annealing greatly increased the mechanical properties of the green films. A hardness of 5.5 - 6.6 GPa (TiO<sub>2</sub>), excellent adhesion and very ductile behavior during scratch tests were found from nanoindentation and scratch tests. Nb<sub>2</sub>O<sub>5</sub> and ZrO<sub>2</sub> thin films were crystalline and stoichiometric, but the higher annealing temperature (600°C), chosen based on DTA/TG measurements, lead to grain growth and deteriorated performance in scratch tests, requiring further optimization.

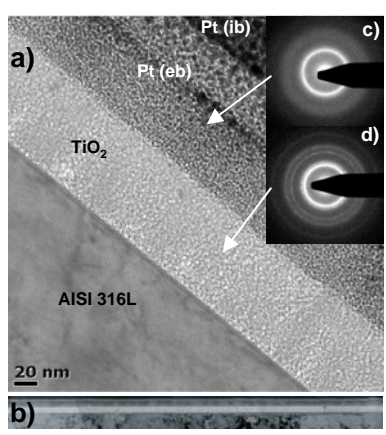


Fig. 1(a) TEM micrograph of annealed electrolytic  $TiO_2$  film on AISI 316L. (b) Overview of thickness uniformity.

**DISCUSSION & CONCLUSIONS:** Based on thickness uniformity, high purity and good mechanical properties, electrolytic TiO<sub>2</sub> films are not only attractive as biocompatible colored coatings on non-anodizable biomedical alloys such as AISI 316 and CoCrMo, but also for Ti-alloys that are often anodized for protective as well as coding reasons prior to implantation.

**REFERENCES:** <sup>1</sup> I. Zhitomirsky, *J. Europ. Ceram. Soc.*, 19, (1999) 2581. <sup>2</sup> P. Kern et. al, submitted to *Thin Solid Films*, (2005).

**ACKNOWLEDGEMENTS:** M. Aeberhart for help with GDOES calibration, Ch. Jäggi for Raman measurements.

### A High-Throughput-Screening Approach for Surface Morphology -Easy way to the cell's preferred topography?

T.P. Künzler, T. Drobek, N.D. Spencer

LSST (Laboratory for Surface Science and Technology), ETH Hönggerberg, Zürich, Switzerland

INTRODUCTION: Surface morphology plays an important role in cell growth, proliferation and attachment to the surface [1,2]. Cells behave differently on smooth surfaces compared to rough ones, but also different kinds of cells favour surfaces with different roughness. However, investigations considering the effect of morphology are often limited to either rough or smooth surfaces. The aim of the current work is to develop roughness gradient surfaces for studying cell-surface interactions of types in vitro specific cell experiments systematically. Characterization of the gradients will be performed by SEM, stereo-SEM and laser profilometry.

METHODS: Morphology gradients were fabricated using a two-step roughening and smoothening process. In a first step, pure aluminium sheets were bead blasted using spherical ceramic beads with a diameter of 125-250 micrometers. With this blasting process a homogeneous roughness was created. In a subsequent chemical polishing process, the sheet was immersed into a hot acidic solution, consisting of phosphoric, nitric and sulphuric acid [3], and continuously withdrawn by means of a linear motion drive. The polishing solution, depending on the residence time of a specific surface location, preferentially removed features with a small radius of curvature and thus led to the smoothing out of the surface topography.

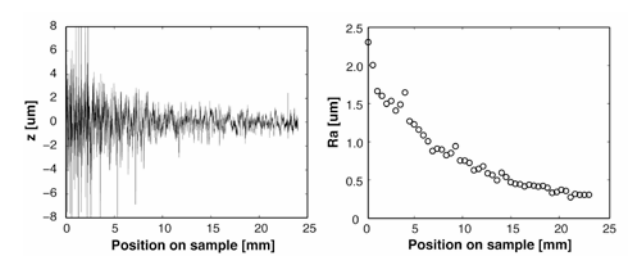


Fig. 1: Laser profilemetry measurements: Profile of the roughness gradient, showing the maximal amplitude (left), calculated roughness values Ra along the gradient axis (right).

**RESULTS:** Following the gradient axis from rough to smooth, the roughness was found to decrease monotonically (Figure 1). Calculations of the standardized integral roughness values from data obtained with laser profilometry showed values of 2.3 micrometer for Ra (arithmetic average) and 3.4 micrometer for Rg (root mean square roughness) at

the rough end and 0.3 micrometer and 0.4 micrometer at the smooth end of the gradient (Figure 1). Figure 2 shows SEM images of the roughest and the smoothest part of the gradient. From studies with the SEM it is revealed that after short polishing time only very small features were removed whereas after polishing the sample for longer time also larger features were removed. This observation could be quantitatively confirmed by stereo-SEM measurements.

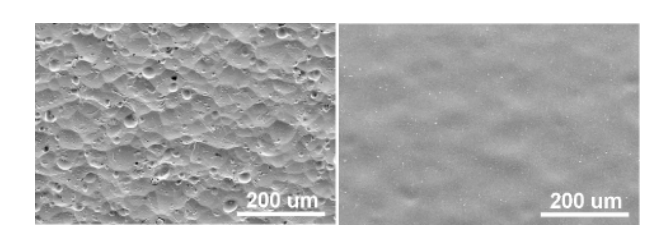


Fig. 2: SEM image of the bead blasted (left) and the polished part (right) of the gradient.

**DISCUSSION & CONCLUSIONS:** The method presented in this work allows for the production of well-defined surface morphology gradients on a centimeter scale with topographical features in the micrometer and sub-micrometer range. Typically, roughness values (Ra) of surfaces used in cell studies lie between 0.2 micrometer for polished and 3.4 micrometer for blasted surfaces [4]. A roughness gradient produced with the presented method covers most of the roughness values in-between this range on a single surface.

**REFERENCES:** <sup>1</sup> G. Abrams, et al (1998) Effects of Substratum Topography on Cell Behavior in *Biomimetic Materials and Design*, Springer, pp 91-137 <sup>2</sup> R. Flemming, et al (1998) *Biomaterials* **20**: 573-588 <sup>3</sup> S. Wernick, et al (1987) Chemical polishing in *The surface treatment and finishing of aluminium and its alloys* Vol.1, ASM International, pp 95-154 <sup>4</sup> K. Anselme, et al (2000) *J Biomed Mater Res* **49**: 155-166

**ACKNOWLEDGEMENTS:** The authors would like to acknowledge C.M. Sprecher and R.G. Richards (AO Research Institute, Davos, Switzerland) for their assistance with SEM. This work was supported by the Swiss National Science Foundation (SNF).

### **Polyelectrolytes on Surfaces**

V.Malinova, C.Wandrey

Faculty of Basic Science, Institute of Chemical and Biological Process Science,
Swiss Federal Institute of Technology
CH-1015 Lausanne, Switzerland

**INTRODUCTION:** Adsorption of charged macromolecules, polyelectrolytes, on oppositely charged surfaces is important for many technical applications including surface and material modification as well as separation of biomolecules. Furthermore, life processes are affected by such electrostatic interactions.

For the adsorption of highly charged cationic polyelectrolytes on oppositely charged porous materials and on oppositely charged Langmuir monolayers the influence of molecular and electrostatic characteristics has been studied. These included the molecule size, the chemical structure and the ionic strength of the medium.

**METHODS:** Poly(vinylbenzylammonium chloride) (PVBAC) samples were synthesized and characterized as described previously [1, 2].

Porous surfaces: Adsorption isotherms have been monitored using strong acidic cation-exchange microspheres of PS-DVB. Two techniques were applied, which yielded the adsorbed amount: adsorption on materials packed in chromatography columns [2] and adsorption on microspheres suspended in aqueous medium.

Langmuir monolayers: The model polyelectrolytes were adsorbed on monolayers of dimyristoylphosphatidic acid. [3].

**RESULTS:** As an example, Fig. 1 illustrates experimental results on porous surfaces, the tendencies of the adsorption behavior influenced by the ionic strength.

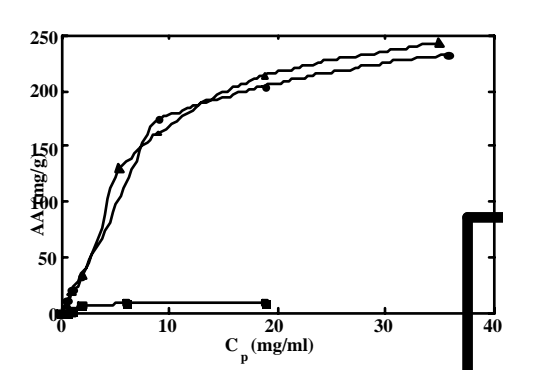


**Fig. 1.** Adsorbed amount, AA, vs. initial polyelectrolyte concentration,  $C_p$ , in: (v) water, ( $\sigma$ ) 0.075 M NaCl, ( $\lambda$ ) 0.225 M NaCl.  $T=25^{\circ}C$ .

Adsorption on porous surfaces: Electrostatic exclusion, in addition to size exclusion, was quantitatively proved evaluating molecular, electrostatic and geometrical parameters (Fig.2).

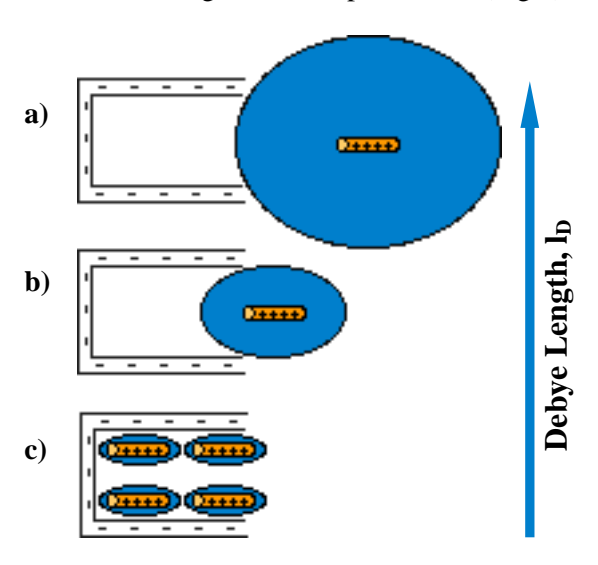


**Fig. 2.** Model proposed to illustrate the adsorption of molecules with L=6 nm on microsphere with  $d_p=10$ -14 nm in water: **a**)  $C_p=0.5$  mg/ml,  $l_D=14.6$  nm; **b**)  $C_p=6$  mg/ml,  $l_D=4.2$  nm, and in 0.075M NaCl: **c**)  $C_p=2$  mg/ml,  $l_D=1.1$  nm. (L=contour length,  $d_p=$ pore diameter,  $l_D=$ Debye length)

Adsorption on monolayers: Pressure-area and pressure-time isotherms revealed an increase of both the area per amphiphile molecule and the surface pressure as a function of time if the polyelectrolyte adsorbs on the amphiphile. Size dependent incorporation of the hydrophobic substituents into the monolayer and end group effects are suggested as the reason for differing monolayer extension.

REFERENCES: [1] W.Jaeger, U.Wendler, A.Lieske, J.Bohrisch, C.Wandrey (2000) *Macromol. Symp.* **161**, p.87-96 [2] V.Malinova, R.Freitag, C.Wandrey (2004) *J. Chromatogr. A* **1036**, p.25-32 [3] V.Malinova, H.Menzel, C.Wandrey (2004) *Progress of Colloid and Polymer Sci.* **129**, p.1-8

**ACKNOWLEDGEMENTS:** The Swiss National Science Foundation is gratefully acknowledged for the financial support, grants: 2100-611314 and 2000 20-101652.

### **DISCUSSION & CONCLUSIONS:**

### **Brushite conversion into apatite**

A.Malsy<sup>1</sup>, M.Bohner<sup>1</sup>

<sup>1</sup> Dr Robert Mathys Foundation, Bettlach, Switzerland.

INTRODUCTION: Calcium phosphate cements (CPC) were discovered by Brown and Chow in the 1980's [1]. Based on the final formulation, two main categories of CPCs are distinguished: (i) apatite and (ii) brushite CPCs. Brushite cement is of special interest due to its good biocompatibility and its large resorption rate. However, in vitro and in vivo results have shown that brushite tends to convert into apatite over time. This conversion is undesirable as resorption rate of apatite is reduced and furthermore this reaction releases acidic phosphate ions which may result in inflammatory reactions. Presently, there is no model to study the conversion rate of brushite cement into apatite. So, the first goal of this study is to establish such a model, whereas the second goal is to assess the effect of various magnesium salts on the stability of brushite cements.

**METHODS:** A powder mixture of basically 10.00g β-tricalcium phosphate (β-TCP), 5.00g monocalcium phosphate monohydrate, 0.187g di-sodium dihydrogen pyrophosphate, and 0.187g sodium sulphate was mixed with 7.5mL 0.5% sodium hyaluronate. In the sample containing Mg salts, either  $0.75g \text{ MgHPO}_4 \cdot 3H_2O$  [2] or  $0.75g \text{ Mg}_3(PO_4)_2 \cdot 8H_2O$ were added to the powder. More sodium hyaluronate solution was added to keep the liquid to solid ratio constant. The cement was mixed for 45sec and cylindrical forms were filled up. Samples were kept at 37°C for one hour and for two additional hours at room temperature. Thereafter, samples extracted and incubated at a temperature of 60°C in 10mL phosphate buffer solution (PBS) (4.5g/L NaCl, 1.788g/L KH<sub>2</sub>PO<sub>4</sub>, and 9.00g/L Na<sub>2</sub>HPO<sub>4</sub>·2H<sub>2</sub>O). After a given incubation time, i.e. 1, 2, 4, 8 days, 2, 4, 6 weeks, only one sample of each composition was taken out of PBS and dried. For the remaining samples PBS was exchanged. pH value as well as calcium ion concentration of the incubation buffer were measured by a pH/ion analyzer. The cylindrical samples were tested mechanically and finally half of each sample was used for X-ray diffraction (XRD) analysis, the other half for scanning electron microscopy (SEM).

**RESULTS:** The pH values increase from pH 6-6.5 after one day to pH 7.3 beyond one day and then drop again at later time down to about pH 6-6.5. The position of the pH drop depends on composition: it occurs after 4, 8 and 14 days for cements without Mg salt, with MgHPO<sub>4</sub>·3H<sub>2</sub>O and with Mg<sub>3</sub>(PO<sub>4</sub>)<sub>2</sub>·8H<sub>2</sub>O,

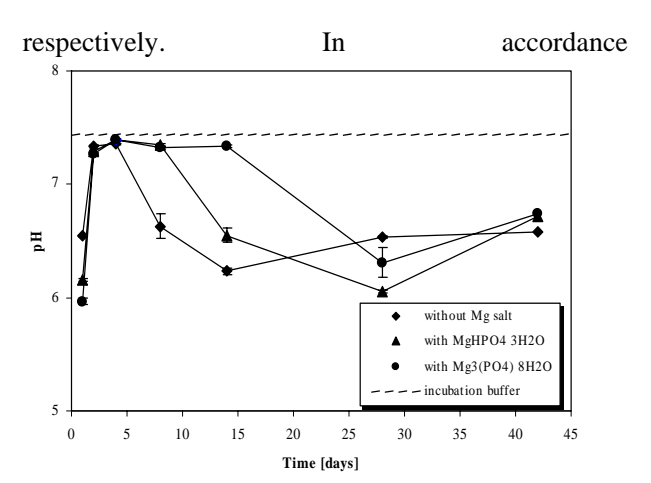


Fig. 1: pH measurements of the PBS. The buffer was renewed after each pH measurement.

to pH measurements XRD analyses showed that in magnesium free formulation. brushite disappeared in favour of octocalcium phosphate (Ca<sub>8</sub>H<sub>2</sub>(PO<sub>4</sub>)<sub>6</sub>·5H<sub>2</sub>O; OCP) and apatite, whereas β-TCP and little apatite were detected in the presence of magnesium salts. SEM photos showed that brushite crystals were more idiomorphic and larger in the absence of Mg salt. A change of microstructure was also observed during the pH drop: spearhead shaped brushite crystals were replaced by platelike or needlelike crystals (for samples containing MgHPO<sub>4</sub>·3H<sub>2</sub>O and Mg<sub>3</sub>(PO<sub>4</sub>)<sub>2</sub>·8H<sub>2</sub>O, respectively). The mechanical properties dropped with an increase of incubation time. Generally, lower values were measured with MgHPO<sub>4</sub>·3H<sub>2</sub>O and Mg<sub>3</sub>(PO<sub>4</sub>)<sub>2</sub>·8H<sub>2</sub>O than without Mg salt.

**DISCUSSION & CONCLUSIONS:** The initially low pH values are due to residual acidity of the cement composition. The pH drop is attributed to the release of acid following the conversion of brushite into a CaP phase with higher Ca/P molar ratio. OCP is known as transient intermediate in the precipitation of the thermodynamically more stable apatite. However, the presence of Mg ions appears to suppress the growth of OCP and favour that of Mgsubstituted  $\beta$ -TCP. The model is adequate because the conversion of brushite into apatite already started after 4 days of incubation. The disappearance of brushite and the precipitation of OCP, apatite or Mgsubstituted β-TCP could be well detected by a combination of pH measurements, XRD analyses, and SEM observations.

**REFERENCES:** <sup>1</sup> W. Brown, L. Chow (1985) *US Patent No.* 4518430. <sup>2</sup> D. Apelt et al (2004) *Biomaterials* **25**[7-8]:1439-51.

### Effect of metal implant surface on fibroblast behaviour

DO.Meredith<sup>1,2</sup>, L. Eschbach<sup>3</sup>, MO.Riehle<sup>2</sup>, ASG.Curtis<sup>2</sup>, RG.Richards<sup>1</sup>

<sup>1</sup>AO Research Institute, Davos-Platz, CH. <sup>2</sup>Centre for Cell Engineering, , University of Glasgow, Glasgow G12 8QQ, UK. <sup>3</sup>Robert Mathys Foundation, Bettlach, CH.

**INTRODUCTION:** Osteosynthesis implant manufacturers offer a selection of metals for internal fracture fixation plates, such as stainless steel (SS), 'commercially pure' titanium (CpTi) and Ti-6% Al-7% Nb (TAN). Comparisons are difficult as the surface finish of the materials vary considerably. 'Standard' SS has a smooth electropolished 'mirror like' finish while cpTi (TS) and TAN (NS) are roughened for enhanced osseointegration. This investigation utilised the standard material finishes and electropolished variants of cpTi (TE) and TAN (NE). These aided in distinguishing between material and topography effects. A form of roughened SS was not included as its reduced corrosion resistance rendered it biologically and commercially Fibroblasts are the major cellular constituent of the adjacent soft tissue fibrous connective tissue therefore our in vitro model of soft tissue interaction uses human fibroblast cell line (hTERT-BJ1).

**METHODS:** Surface characterisation performed using Atomic Force Microscopy (AFM), Profilometry and Scanning Electron Microscopy (SEM). Cell reactivity distinguished into qualitative and quantitative assessment. Qualitative assessment utilised SEM for cell growth and morphology at 24h, 5 and 10d timepoints. Intracellular components, vinculin, tubulin, actin and DNA, were fluorescently labelled and imaged using the Fluorescence Microscope (FM) at 48h. DNA from cells cultured for 24h, 5 and 10d was extracted and quantified to confirm qualitative cell growth findings.

RESULTS: SS, TE and NE were all smooth samples with Ra's between 0.18-0.19μm. While similar in Ra, AFM and SEM demonstrated that all materials had some variation in topography. SS had some surface scratches, TE had a topography of nanometric surface nodules and NE displayed an undulating topography. The rougher materials, TS and NS had higher but similar Ra's of 0.90 and 0.77μm. AFM and SEM demonstrate that the similarities end here with TS having a rugged irregular surface, and NS demonstrating a 'microspiked' topography consisting of protruding particles. Qualitative cell growth on the samples, by SEM, demonstrates that cells reached confluency by the 10d timepoint on all samples

except NS. This growth suppression confirmed to a level of statistical significance by DNA quantification. (P>0.01)morphologies were well spread on SS, TE and NE at both 24h and 5d timepoints. The morphology only changed due to lack of surface space, and cells adopted an elongated morphology. Cells on TS were not well spread at 24h with investigatory filopodia emanating from far from the cell body. By 5d, cells were better spread and 10d were elongated with confluent numbers. On NS, cells at all timepoints were rounded or elongated. At 24h and 5d filopodia could be seen attaching to the microspikes, however by 10d this exploration had ceased. On some cells, membrane integrity was reduced to a much coarser texture indicative of cell necrosis. Intracellular labelling demonstrated that on SS, TE and NE the focal adhesion (FA) sites were mature with associated actin cytoskeleton and a well conserved microtubule network. On TS, cells were less spread with smaller FA but a wellconserved actin and microtubule network. For NS, cells were again unspread and FA's were small and could be observed avoiding the microspikes. The underlying microspikes could also be seen actively impairing for formation of the microtubule network.

**DISCUSSION & CONCLUSIONS:** Our findings indicate that surface chemistry is not paramount to cytocompatibility. NE's bio-performance (with regards to fibroblasts) was exceptional in comparison with its material counterpart, NS. A general roughened topography was also not the cause as both TE and TS performed well. As can be seen from the interaction of the filopodia, FA's and microtubules, the additional factor of NS is its unique microspiked topography. These are β-phase particles of titanium, an inherent characteristic of the TAN microstructure. They are also present in a smoothed form in NE but are of no significance to cytocompatibility. We propose topographical presence and dimensions of the particles inhibits the spreading of cells and development of mature FA's; two essential factors in the progression of the cell cycle and cell growth.

New in vitro technique for the evaluation of prostheses: Dynamic fatigue combined with crevice corrosion

<u>L. Reclaru<sup>1</sup>, L.Reto<sup>2</sup></u>, PY Eschler<sup>1</sup>, M. Zuberbühler<sup>2</sup>, A. Blatter<sup>1</sup>, P.Wehrli<sup>2</sup>

<sup>1</sup> PX Holding SA La Chaux-de-Fonds Switzerland. <sup>2</sup> Plus Orthopedics AG Rotkreuz Switzerland

**INTRODUCTION:** An electrochemical study of the corrosion resistance of the articulation interface (distal / proximal module) of a prosthesis was performed in combination with a cyclic fatigue test. The complexity of the situation resides in the existence of interfaces between the distal part, the proximal part, and the dynamometric screw. A new technique for the evaluation of the resistance to cyclic dynamic corrosion with crevice stimulation of modular prostheses is presented. Two components of explanted modular prostheses of the same type after cyclic dynamic test with stimulation of crevice corrosion

**METHODS:** The test samples are complete modular prostheses. The distal module of the prosthesis was embedded in a reactive resin. The electrochemical cell was equipped with a Luggine capillary for the reference electrode (Fig.1 and 2)





The potentiostatic technique was adopted from the ASTM F746-97 standard. The test was conducted in steps of one million cycles for a total of 5 million fatigue cycles, and 200 potentiostatic (electrochemical) cycles were measured during the 5 million mechanical fatigue cycles. The procedure of a potentiostatic cycle consisted in stimulating at a potential of 800 mV SCE for 60 seconds and then recording the current at preselected potentials of 600 mV , 650 mV , 700 mV and 750 mV vs SCE for 36 minutes at each increment.

The test milieu was a solution of NaCl at a concentration of 9 g/l in ultra-pure water.

**RESULTS:** The integration of the potentiostatic curves gives the quantities of electrical charge (in microcoulombs) consumed in the fatigue process at each preselected potential. Fig. 3 displays the entirety of these results.

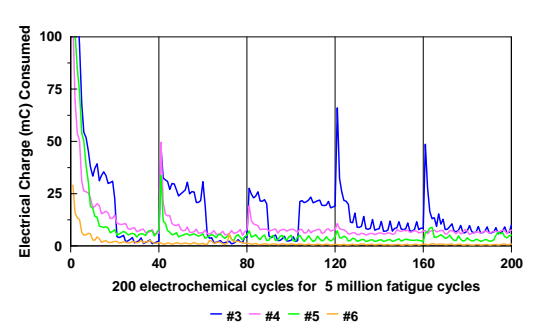


Fig 3 Behaviour of localised corrosion of prostheses #3, #4 and #5 (series1) during 5 million mechanical fatigue cycles.

### **DISCUSSION & CONCLUSIONS:**

According to the results obtained, the evaluated electrochemical parameters and the visual observations reveal that:

- 1) The electrolyte penetrates into the interface of the distal/proximal modules during cyclic dynamic tests; this is not the case during static electrochemical tests.
- 2) The distal module undergoes cracking and corrosion in the interface region

A comparison of the explanted proximal parts with modular prostheses of the same type evaluated during the cyclic dynamic tests with stimulation of crevice corrosion, show significant similarities with regard to the phenomena of electrolyte diffusion, deposition of products and corrosion (Figs 4 and 5).



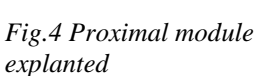




Fig.5 proximal module #4 evaluated in fatigue test

These observations motivate the use of comparative cyclic dynamic tests with stimulation of crevice corrosion in the design and evaluation stage of modular prostheses.

# Analysis of laser welded joints on "C" alloy used in the removable partial dentures technology

Cristina Bortun<sup>1</sup>, Ion Mitelea<sup>2</sup>, Livius Milos<sup>2</sup>, Valentin Bîrdeanu<sup>3</sup>, Liliana Sandu<sup>1</sup>

<sup>1</sup> "Victor Babeş" University of Medicine and Pharmacy, University Dental College, Spl. T. Vladimirescu nr. 14, Timişoara, România

**INTRODUCTION:** The quality of laser welded joints of some alloys used in dental technology can be evaluated by destructive and nondestructive testing methods. Some of the destructive testing methods are: metallographic analysis and microhardness testing and non-destructive methods are: spectrographic and radiographic analyses [1,2,3].

**METHODS:** Some "C" alloy plates, Cr-Co-Mo type (VASKUT KOHASZATI KFT), were cast by various thicknesses, between 0.4 and 1mm. The plates were welded in a configuration butt joint, using a Nd:YAG laser (table nr. 1). The welded samples were prepared for metallographic analysis, microhardness testing and chemical analysis.

Table nr.1: Characteristics of the laser HL 124P LCU (TRUMPF) used in experiment.

P <sub>med</sub> (W)	$P_{p}(KW)$	$P_{p}(KW)$ $t_{p}(ms)$		$E_{p}(J)$
max.120	max. 5	0,3-20	600	0,1-50

### **RESULTS & DISCUSSIONS:**

Figure 1 presents macroscopic aspects and microscopic images of the welded joints.

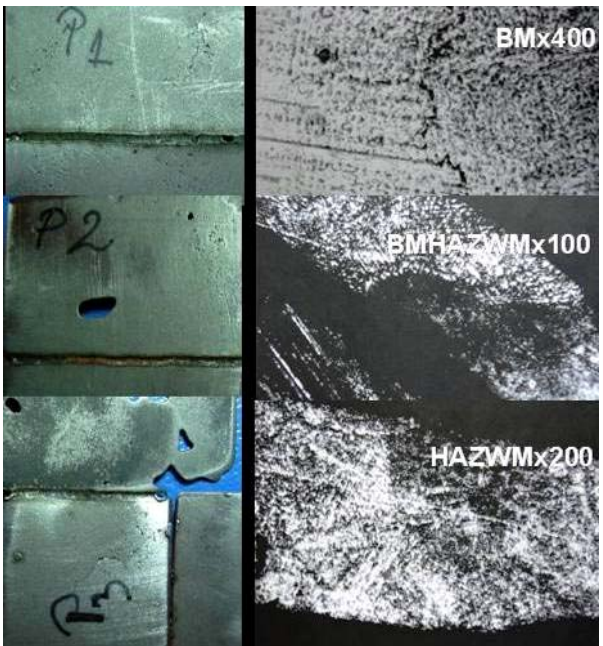
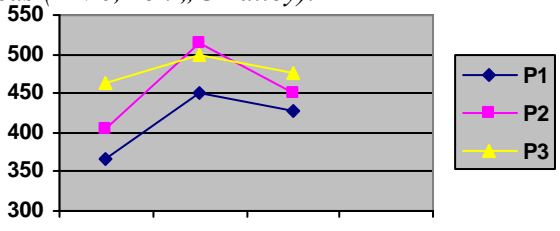


Fig. 1. Macroscopic aspects and microscopic images of the samples P1, P2 and P3.

It can be seen a good commpactity of the welded joints and no continuity defects in the welded zone.

Microhardness analysis made with 100 g charges shows a small increasing of the hardness in HAZ (heat affected zone) and in weld metal (WM) the hardness is between the BM (base metal) and HAZ (fig.2). It were made 5-6 impressions in each zone of the welded joints.

Fig. nr. 2: Microhardness variations in welded areas (HV0,1 on ,, C" alloy).



Related to the chemical composition of the welded areas, it can be seen a small decrease of the main reactive elements (table nr. 2).

Table nr. 2: Chemical composition of the alloy.

Chemical elements	Co (%)	Cr (%)	Mo (%)
BM	65	29	5
WM	64,1	27,4	4,1

#### **CONCLUSIONS:**

- The materials used in dental technology ca be welded by laser (this is also a method of the prostheses repairs).
- The analyses and tests show a good quality of the welded joints.
- In the base material with thickness over 1 mm appear some cracks, cause of casting technology.

REFERENCES: <sup>1</sup> Lindemann W. (2000) Materialkundliche Untersuchungen an Laserschweißverbindungen zwischen Edelmetallund Nichtedelmetalllegierungen, dental/labor, XLVIII, H2, pg. 199-202. <sup>2</sup> Schneidenbanger T. (2000) Der Einsatz des Lasers am Beispiel eines Klammerbruchs, dental/labor, XLVIII, H2, pg. 207-209. <sup>3</sup> Lindemann W. (2004) Plasma versus Laser, dental/labor, LII, H5, pg. 793-799.

<sup>&</sup>lt;sup>2</sup> Politehnica University, Mechanical Engineering Faculty, Bd. Mihai Viteazul I, Timişoara, România <sup>3</sup>National R&D Institute for Welding and Material Testing, Bd. Mihai Viteazul 30, Timişoara, România

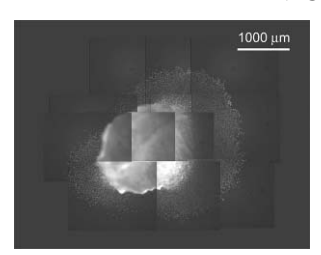
# Primary Osteoblasts Outgrown from Rat Calvarial Explants Form a "Fried-egg"-like Image on Non-fouling Peptide-modified Titanium Surfaces

M. Schuler<sup>1</sup>, S. Tosatti<sup>1</sup>, D. W. Hamilton<sup>2</sup>, C. M. Sprecher<sup>3</sup>, M. deWild<sup>4</sup>, D. M. Brunette<sup>2</sup>, M. Textor<sup>1</sup>

<sup>1</sup>Dept. of Materials, Federal Institute of Technology (ETH), Zurich, Switzerland, <sup>2</sup>Dept. of Oral Biological & Medical Sciences, University of British Columbia, Vancouver, B.C., Canada, <sup>3</sup>AO Research Institute, Davos, Switzerland, <sup>4</sup>Institut Straumann AG, Basel, Switzerland

**INTRODUCTION:** A new trend in fabricating proactive implant surfaces is the immobilization of peptide sequences that mimic proteins found within the extracellular matrix (ECM). Such bioligands have the ability to bind to the cell via specific cell surface receptors. The RGD sequence is the most prominent ligand addressing integrins, a family of receptors present in most cell types. Other sequences such as KRSR and FHRRIKA bind transmembrane proteoglycans (e.g. heparan sulfate). These peptide patterns are found in the ECM of osteoblasts<sup>1, 2</sup> and are therefore similarly interesting for bone-contact applications. Our concept of immobilizing bioactive molecules is based on poly-L-lysine-g-poly(ethylene glycol) (PLL-g-PEG) adlayers<sup>3</sup>. The dense PEG brush creates a non-fouling biomaterial surface to prevent non-specific protein adsorption and is further modified by coupling the peptide sequences containing RGD, KRSR or FHRRIKA.

**METHODS:** SLA commercially pure titanium discs (sand-blasted and acid-etched; Straumann AG, Switzerland) were coated with peptide-modified PLL-*g*-PEG. Bone chips (2 mm in diameter) were punched from calvarial bone of newborn rats (Sprague Dawley) and placed onto the coated Ti surfaces (figure 1).



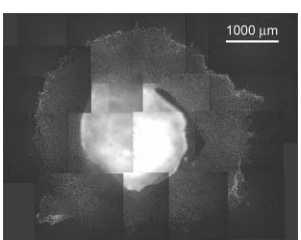


Fig. 1: Fluorescent images showing a bone chip from rat calvaria surrounded with outgrown osteoblasts. Left panel: non-functionalized PLL-g-PEG modified Ti surface; right panel: KRSR peptide-modified PLL-g-PEG Ti surface.

Chips were fed after 4 days every second day using media supplemented with ascorbic acid and  $\beta$ -glycerophosphate. Outgrown cells were fixed with 4% formaldehyde/PBS and the nuclei stained with DAPI for fluorescence investigation.

**RESULTS:** None of the bone chips stuck after 4 days of incubation, although few cells grew out of the bone. After 6 days, bone chips attached to the surfaces and cells migrated in a circular way building up a "fried-egg"-like image (Fig. 1). Cells on non-functionalized PLL-*g*-PEG covered a significant smaller area than cells on all the other surfaces (Fig. 2) and were also the only ones that did not migrate out in an isotropic way (Fig. 1, left panel).

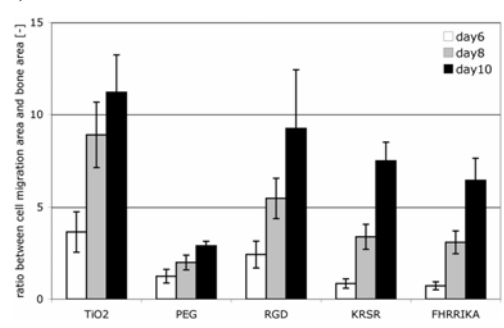


Fig. 2: Ratio between the area covered by outgrown rat calvarial osteoblasts and the bone chip area. Peptide density was 3.0 pmol/cm<sup>2</sup>.

DISCUSSION & CONCLUSIONS: Experiments using explants are closer to *in vivo* experiments than standard *in vitro* cell culture assays and they have the advantage of using "real" primary cells at low cell cycles. Coating Ti implant surfaces with the osteoblast-selective peptides KRSR and FHRRIKA appears to be promising, although they do not reach the efficiency of the RGD peptide surfaces at equal peptide surface densities. However, the use of their specificity of addressing cell surface receptors found in osteoblasts is a useful approach for novel biomaterial surfaces.

**REFERENCES:** <sup>1</sup>Dee, K.C. *et al.*, J Biomed Mater Res, 40(3): p. 371-377, 1998. <sup>2</sup>K. E. Healy *et al.*, Bioartificial Organs Ii: Technology, Medicine, and Materials, p. 24-35, 1999. <sup>3</sup>Tosatti, S., *et al.*, J Biomed Mater Res, 68A(3): p. 458-472, 2004.

**ACKNOWLEDGEMENTS:** This project was supported by the ITI Foundation for the Promotion of Oral Implantology and by the Swiss Federal Commission for Technology and Innovation CTI (both Switzerland).

# Water sorption of some experimental dental composites based on (modified-Bis-GMA) superior olygomers

C. Tamas, C. Prejmerean, M. Moldovan, A. Colceriu, L. Vezsenyi, G. Furtos, D. Prodan

<sup>1</sup> "Raluca Ripan" Chemistry Research Institute, 30 Fantanele Street, 400294, Cluj-Napoca, RO

**INTRODUCTION:** Starting from the idea that the transformation of the hydroxy groups of the Bis-GMA<sub>0-2</sub> superior olygomers in methacryloyl-oxy groups leads to the obtaining of olygomers with low viscosity and respectively to dental resin composites with low water sorption [1]. The paper studies the synthesis of modified Bis-GMA superior olygomers and their influence upon the water sorption of the corresponding experimental dental composites.

METHODS: 1.The synthesis of (modified Bis-GMA<sub>0-2</sub>) superior olygomers. A mixture of olygomers called (modified Bis-GMA)<sub>0-2</sub> has been synthesized using the mixture of three components Bis-GMA<sub>0-2</sub> having 83 mol % Bis-GMA<sub>0</sub> monomer- 2,2-bis[4-(2-hydroxy-3-methacryloyloxypropoxy)phenyl]-propane-, 16 mol % Bis-GMA<sub>1</sub> dimer, 1 mol % Bis-GMA<sub>2</sub> and methacryloyl chloride.

for n=0 Bis-GMA<sub>0</sub> $\rightarrow$ (modified Bis-GMA)<sub>0</sub>

n=1 Bis-GMA<sub>1</sub> $\rightarrow$  (modified Bis-GMA)<sub>1</sub>

n=2 Bis-GMA<sub>2</sub> $\rightarrow$  (modified Bis-GMA)<sub>2</sub>

Fig. 1 The synthesis of the (modified Bis-GMA)<sub>0-2</sub> olygomers

**2.Obtaining of the experimental composite resins.** A series of 5 light-curing experimental composites based on different monomer mixtures containing (Bis-GMA)<sub>0-2</sub> and (modified Bis-GMA)<sub>0-2</sub> superior olygomers with the diluting monomer, triethyleneglycole dimethacrylate (TEGDMA) have been prepared. The inorganic filler consisted of 90% silanized SrO glass and 10% silanized colloidal silica. The powder/liquid ratio was 4/1.

### 2. Determination of the water sorption

The method for evaluating the water sorption was in accordance to ISO 4049/2000.

**RESULTS:** Using IR spectroscopy, the total transformation of the Bis-GMA<sub>0-2</sub> olygomers was demonstrated and the double bonds content of the reaction product, (Bis-GMA modified)<sub>0-2</sub>, was determined as 22.7% H<sub>2</sub>C=C(CH<sub>3</sub>) groups. By correlating the HPLC chromatogram of the reaction product (modified Bis-GMA)<sub>0-2</sub> with the value obtained for the double bonds from the IR spectrum, the composition of the olygomer mixture (modified Bis-GMA)<sub>0-2</sub>: 82.1% (modified Bis-GMA)<sub>1</sub> was established. The compositions of the Bis-GMA)<sub>1</sub> was established Bis-GMA)<sub>0-2</sub>/ TEGDMA monomer mixtures and the properties of the corresponding composites are presented in the table 1.

Table 1

	Sample 1	Sample 2	Sample 3	Sample 4	Sample 5
Monomers ratios					
Bis-GMA <sub>0-2</sub> /	10/	20/	30	40/	45/
(modified Bis-GMA) <sub>0-2</sub>	40/	30/	20/	10/	5/
/TEGDMA	50	50	50	50	50
Water sorption, µg/mm <sup>3</sup>	22,05	27,63	29,90	32,44	35,84

**DISCUSSION & CONCLUSIONS:** The water sorption decreases with the increasing of the (modified Bis-GMA)<sub>0-2</sub> in the mixture because of the hydrophobic character of the (modified Bis-GMA)<sub>0-2</sub> olygomers and of the high crosslinking density of the resulted polymer network.

**REFERENCES:** <sup>1</sup>C.Prejmerean, M. Moldovan, M. Brie, G. Furtos, D. Prodan, (2001), Revue de Chemie, **52(9)**: 500-506

# COMPARATIVE S.E.M. OBSERVATION OF CLASSICAL AND BONDED AMALGAM RESTORATIONS

I.A.Tig<sup>1</sup>, O.Fodor<sup>1</sup>, M.Moldovan<sup>2</sup>

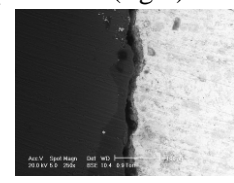
<sup>1</sup> University of Oradea, Romania, Faculty of Medicine and Pharmacy, <sup>2</sup> Institute of Chemistry Research "Raluca Ripan" Cluj-Napoca, Romania

INTRODUCTION: Dental amalgam has passed the "time test" for over 150 years as a strong, durable and relatively inexpensive restorative material. However, recently, a strong wave of "anti-amalgamists" is trying to rid amalgam because of disadvantages including microleakage, lack of adhesion to tooth structure or sensitivity. Amalgam bonding agents and new amalgam alloys were developed to address these concerns. In this study we compared the SEM images of the amalgam-tooth structure interface in different types of classical and bonded amalgam restorations.

**METHODS:** Freshly extracted non-carious premolars and molars were collected and stored in distilled water. Each tooth was prepared as followed: ideal class I cavities preparations were performed using a water-sprayed, high-speed handpiece with new diamond-coated burs. Each cavity was cleaned and dried. We used two types of alloys: Lojic+ (SDI Australia) - a single composition spherical alloy, and Ultracaps+ (SDI Australia) – an admix alloy of spherical and irregular particles. For each alloy type we prepared a "witness" tooth: amalgam was triturated with Ultramat2 amalgamator (SDI Australia), according to manufacturer's instructions, and then condensed into the prepared cavity using a double-ended amalgam carrier and amalgam plugger. After carving to anatomic contour, the amalgam was left for 24 hours in distilled water for final setting and than burnished.

OptiBond Solo Plus (Kerr) single bottle bonding agent was used for amalgam bonding in the test sample. The bonding agent was applied according to manufacturer's instructions, prior to amalgam condensation. All teeth were then vertically sectioned into 3 mm thick halves with water-cooling, using a precision cutting instrument with a diamond disc. After cleaning, the samples were stored in distilled water and examined in various magnifications under the scanning electron microscope.

**RESULTS:** Different areas of the specimens were in observed under the S.E.M. magnifications. It was noticed that, at lower rate of magnification. there no significant were differences between classical and bonded amalgam, regardless of the alloy type used. At higher rate of magnification we can see that the teeth restored with unbonded amalgam ("witness" specimen) had more spaces and artifacts at the amalgam-tooth structure interface, spaces that are filled with bonding agent in the case of test specimens (fig.1).



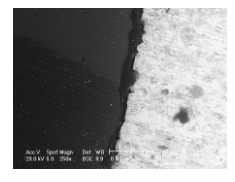


Fig. 1: Unbonded (left) and bonded (right) amalgam fillings (magnification 250X).

**DISCUSSION & CONCLUSIONS:** Studies have shown that the resultant retention with amalgam bonding is equal to or superior to the traditional means of mechanical retention<sup>1</sup>. Also, a reduction in sensitivity and a more conservative cavity preparation can be achieved when amalgam is bonded to a tooth<sup>2</sup>. Studies to examine the efficacy of single-bottle bonding agents for use in amalgam bonding have been made<sup>3,4</sup>.

In this study, interfaces of teeth restored with bonded amalgam based on different types of alloy, using a single-bottle bonding agent, were observed under the S.E.M.. The photomicrographs show that tooth restored with unbonded amalgam had more spaces and artifacts at the amalgam-tooth structure interface than the tooth restored with a bonded amalgam.

Further research must be done to verify the sealing abilities and bonding strength of the different single-bottle bonding agents when used in amalgam bonding in association with different types of amalgam alloys.

### **REFERENCES:**

<sup>1</sup>.Staninec M. Retention of amalgam restorations: undercuts versus bonding. Quint Int 1989;20:347-351. <sup>2</sup>.Devlin H. New developments in tooth restoration with amalgam. Dent Update 1993; Jan-Feb:21-24. <sup>3</sup>.Cobb DS, Denehy GE, Vargas MA. Amalgam shear bond strength to dentin using single-bottle primer/adhesive systems. A J Dent 1999;12:222-6. <sup>4</sup>.Dhanasomboon S, Nikaido T, Shimada Y, Tagami J. Bonding amalgam to enamel: shear bond strength and s.e.m. morphology. J Prosthet Dent 2001;86:297-303.

### Highly porous silk scaffolds for bone defect repair

L. Uebersax<sup>1</sup>, S.Hofmann<sup>1</sup>, H.Hagenmüller<sup>1,2</sup>, R. Müller<sup>2</sup>, H.P.Merkle<sup>1</sup>, L.Meinel<sup>1,3,4</sup>

<sup>1</sup> Drug Formulation and Delivery, ETH, Wolfgang-Pauli-Strasse 10, CH-8093 Zürich.

<sup>2</sup> Institute for Biomedical Engineering, ETH, Moussonstrasse 18, CH-8044 Zürich

<sup>3</sup> Harvard – M.I.T. Division of Health Sciences and Technology, M.I.T., Cambridge, MA

<sup>4</sup> Department For Bioengineering, Tufts University, Medford, MA

**INTRODUCTION:** The distinguishing features of silk fibroin (SF) matrices as compared to other protein biomaterials revolve around their excellent biocompatibility together with their mechanical properties rivalling even synthetic high performance fibers such as Kevlar. We developed a novel production process for silk scaffolds that is starting off from aqueous SF solutions, whereas earlier methods used organic solutions. Here, we describe the fabrication of SF implants, with a precise control over scaffold porosity and interconnectivity.

**METHODS:** Aqueous silk fibroin solutions were prepared from Bombyx mori cocoons. Briefly, cocoons were washed and dissolved in 9M LiBr and dialyzed under osmotic pressure resulting in 20% (w/w) SF solutions. This solution was transferred into a mold, filled with sieved paraffine globules (porogens). Pore sizes were controlled by globule diameter and interconnectivity by heat treatment of the spheres (prior to adding the SF solution), resulting in a controlled melting of the contacting areas of the paraffin (Heat treatment at 24, 37 and 45°C for 50minutes each). Scaffolds were assessed by SEM and mechanically tested (Zwick 1456). To evaluate cellular responses, SF scaffolds were seeded with human mesenchymal stem cells (MSC). Proliferation was assessed using a Pico Green assay (DNA) and histologically (H&E staining) in control medium (10% FBS in DMEM) and osteogenic responses by u-computed tomography (mineralization and histological evaluation will follow), in osteogenic medium (10% FBS, 10mM μ-glycerolephosphate, 50 μg/ml ascorbic acid-2-phosphate, and 1 µg/ml BMP2.

**RESULTS:** The mechanical properties of the scaffdolds were markedly influenced by implant porosity and pore interconnectivity (**Fig. 1A**). The elastic modulus (2% strain) was higher for scaffolds treated 37°C as compared to 25°C or 45°C. The impact of the pore diameter on mechanical properties was less pronounced with the exception of scaffolds treated at 25°C, when pore sizes between 300 – 400  $\mu$ m resulted in a considerably higher elastic modulus as compared to the other pore sizes (**Fig.1B**). Cell proliferation on the scaffolds was similar as compared to SF

scaffolds prepared form organic SF solutions [1,2], and MSC deposited a network of calcified clusters, more pronounced at the scaffold rim as compared to the scaffold center.

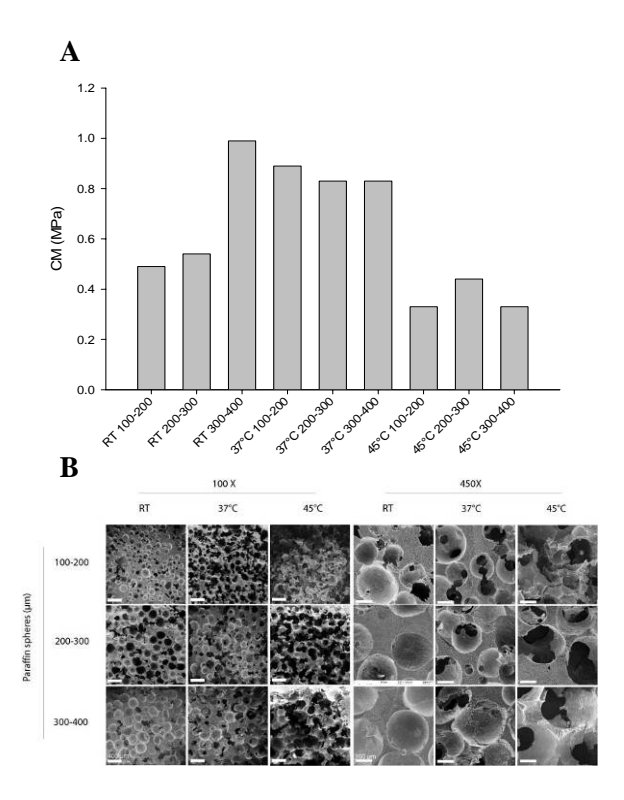


Fig. 1(A): Influence of pore size and interconnectivity on the young's module of silk scaffolds. (B) SEM images taken from scaffolds with different pore sizes and interconnectivity

**DISCUSSION & CONCLUSIONS:** This study describes a novel process for the fabrication of silk implants starting off from aqueous SF solutions, with a precise control over porosity and interconnectivity. Future directions of our research using highly concentrated and aqueous SF solutions direct at expanding the biomedical applications of silks, with a focus on drug formulation and delivery.

ACKNOWLEDGEMENTS: We thank Trudel Inc. (Zurich) for silk cocoons. Financial support was from AO (AO Biotechnology Research Grant 2003), ETH Zurich (TH Gesuch), and the US National Science Foundation (# 0436490).

NTA (nitrilotriacetic acid)-derivatized Poly(L-lysine)-g-poly(ethylene glycol): A Novel Polymeric Interface for Binding and Study of 6xHistidine-tagged Proteins

G.L.Zhen<sup>1</sup>, S.Zürcher<sup>1</sup>, D. Falconnet<sup>1</sup>, E. Kuennemann<sup>2</sup>, J. Vörös<sup>1</sup>, N. Spencer<sup>1</sup>, M. Textor1<sup>1</sup>

Laboratory for Surface Science and Technology, ETH Zurich, Zurich, Switzerland

Institute for Molecular Biology and Biophysics, ETH Zurich, Zurich, Switzerland

**INTRODUCTION:** Interfaces are key elements in the design and fabrication of bioaffinity sensor chips with directed biological response. It has been reported that coating metal oxide surfaces with poly(L-lysine)-*g*-poly(ethylene glycol) (PLL-*g*-PEG) provides an attractive option for producing stable surfaces that are protein-resistant<sup>1</sup>. A novel NTA-functionalized PLL-*g*-PEG is presented that it can assemble on oxide surfaces as a monolayer, allows for the immobilization of proteins through NTA-Ni<sup>2+</sup>-histidine docking site chemistry.

METHODS: Graft copolymer PLL-g-PEG/PEG-NTA was synthesized with a fraction of the PEG chain terminus covalently functionalized with nitrilotriacetic acid (NTA) as a chelating ligand. The polymer was assembled from aqueous solution onto Nb<sub>2</sub>O<sub>5</sub> coated optical chips, followed by coordination of Ni<sup>2+</sup> to the surface-exposed NTA ligand. Subsequently, this sensing platform was used to specifically attach Histidine-tagged 6His-GFP(Green Fluorescent proteins, e.g., Protein) or enzymes, e.g., 6His-β-lactamase. Optical waveguide lightmode spectroscopy (OWLS) was used to monitor quantitatively and in situ for each step. Furthermore, the NTAfunctionalized polymer was used to produce interactive micropatches in a non-interactive PLLg-PEG background on Nb<sub>2</sub>O<sub>5</sub> coated surfaces by a novel approach termed molecular assembly patterning by lift-off (MAPL)<sup>2</sup>. The quality of the 6His-GFP patterns was evaluated by confocal laser scanning microscopy (CLSM).

**RESULTS:** OWLS studies of 6His-GFP bound to NTA-functionalized polymer modified surfaces proved that the binding of 6xHis-tagged proteins was stable and required the presence of Ni<sup>2+</sup> attached to the NTA functionalities. The proteins could be fully removed by exposing the surface to imidazole or EDTA. Non-specific adsorptions of 6His-GFP and 6His-β-lactamase were below 2 ng/cm<sup>2</sup>. Binding and desorption of 6xHis-tagged was repeated in several demonstrating the excellent regeneration capacity of the novel platform (Fig. 1). Fluorescence microscopy measurement proved that patterning was successful and that surfaceimmobilized 6His-GFP was in an active conformation (Fig. 2).

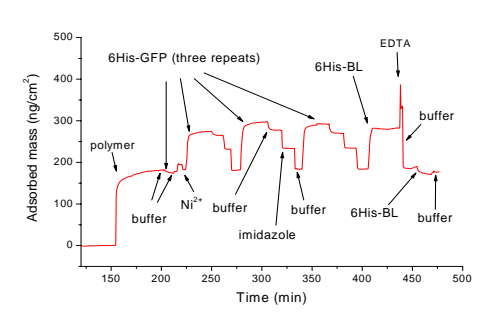


Fig. 1: Adsorbed mass measured by OWLS of the sequential adsorption of PLL-g-PEG/PEG-NTA,  $Ni^{2+}$ , 6His -GFP and 6xHis - $\beta$ -lactamase. Quantitative regeneration of the surface was achieved by adding either EDTA, which removes  $Ni^{2+}$  or imidazole, which removes only the His-tagged protein, but not  $Ni^{2+}$ .

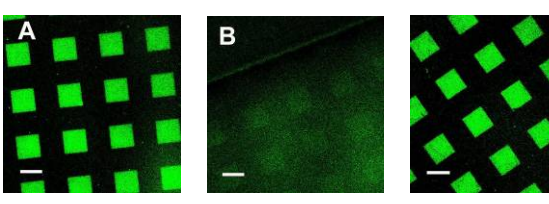


Fig. 2: Pattern of 6His-GFP on  $Nb_2O_5$  analyzed by CLSM. The scale bar represents 60  $\mu$ m. (A) 6His-GFP immobilized on MAPL patterned substrate after charging with  $Ni^{2+}$ . (B) As A, rinsed with imidazole removing 6His-GFP. (C) As B, reloaded with 6His-GFP.

**DISCUSSION & CONCLUSIONS:** We have demonstrated that the novel PLL-g-PEG/PEG-NTA polymeric interface is a promising approach for the binding of 6xHis-tagged proteins in an oriented manner with active conformation. Furthermore, the combination of the MAPL patterning technique with the PLL-g-PEG/PEG-NTA system is considered to be a promising technique for the production of functional microarrays in the area of genomics and proteomics.

### **REFERENCES:**

- (1) Kenausis, G. L.; Voros, J.; Elbert, D. L.; Huang, N. P.; Hofer, R.; Ruiz-Taylor, L.; Textor, M.; Hubbell, J. A.; Spencer, N. D. *Journal of Physical Chemistry B* 2000, 104, 3298-3309.
- (2) Falconnet, D.; Koenig, A.; Assi, T.; Textor, M. *Advanced Functional Materials* 2004, 14, 749-756.